J. Membrane Biol. 33, 141–183 (1977)

Changes in Absorption, Fluorescence, Dichroism, and Birefringence in Stained Giant Axons: Optical Measurement of Membrane Potential

W.N. Ross*, B.M. Salzberg**, L.B. Cohen, A. Grinvald, H.V. Davila***, A.S. Waggoner, and C.H. Wang

Department of Physiology, Yale University, School of Medicine, New Haven, Connecticut, 06510, Department of Chemistry, Amherst College, Amherst, Massachusetts, and The Marine Biological Laboratory, Woods Hole, Massachusetts

Received 13 August 1976

Summary. The absorption, fluorescence, dichroism, and birefringence of stained squid axons were measured during action potentials and voltage clamp steps in an effort to find large optical signals that could be used to monitor membrane potential. Changes in all four optical properties were found that were linearly related to membrane potential and, with several new dyes, the signal-to-noise ratios were larger than any obtained previously. The problem of photodynamic damage was greatly diminished; with a merocyanine-rhodanine dye, the photodynamic damage associated with intense light and the presence of oxygen was negligible. The absorption change obtained with this dye was relatively large; it could be measured with a signal-to-noise ratio of 100:1 during a single action potential.

Changes in light scattering and birefringence that occur during action potentials in unstained axons (intrinsic signals) and changes in the fluorescence of stained axons (extrinsic signals) were first described in 1968 (Cohen, Keynes & Hille, 1968; Tasaki, Watanabe, Sandlin & Carnay, 1968). Further experiments indicated that most of these signals were related to the changes in membrane potential that occur during the action potential (Cohen *et al.*, 1968; Conti & Tasaki, 1970; Cohen *et al.*, 1971; Davila, Cohen, Salzberg & Shrivastav, 1974). Thus these optical signals could, in principle, be used to monitor membrane potential. However, except in the special circumstance where a large membrane area

* *Present address:* Department of Neurobiology, Harvard Medical School, Boston, Massachusetts.

** *Present address:* Department of Physiology and Pharmacology, School of Dental Medicine, and Institute of Neurological Sciences, University of Pennsylvania, Philadelphia, Pennsylvania.

*** *Present address:* Departamento de Fisiologia, Facultad de Medicina, Universidad Los Andes, Merida, Venezuela.

can be studied (e.g., Baylor & Oetliker, 1975), these signals were too small to be of practical value and extensive signal averaging was usually required to detect them. Because optical methods might provide a powerful tool for measuring membrane potential in preparations where the use of electrodes would be inconvenient or impossible, we began a search for larger signals (Cohen, Landowne, Shrivastav & Ritchie, 1970). At that time the largest signal-to-noise ratio obtained during a single action potential in a squid axon was about 1:1.

By testing additional fluorescent dyes, especially merocyanines, cyanines and oxonols (Hamer, 1964), we were able to find a merocyanine dye which gave a signal-to-noise ratio of about 10:1 (Davila, Salzberg Cohen & Waggoner, 1973; Cohen *et al.*, 1974). However, even though the signal with this merocyanine dye was large enough to monitor activity in giant axons, when this dye was added to neurons with a much smaller membrane area, adequate signal-to-noise ratios in a single sweep were achieved only with difficulty (Salzberg, Davila & Cohen, 1973). Therefore, the search for larger signals was continued.

In studies of the origins of the potential dependent changes in fluorescence of cyanine dyes, Sims, Waggoner, Wang and Hoffman (1974) discovered concomitant changes in absorption. Thus, it was expected that absorption changes would be found in experiments on giant axons. The results presented here summarizing absorption and fluorescence measurements on 270 additional dyes confirm that expectation. The absorption change of a merocyanine-rhodanine dye was detected with a signal-to-noise ratio of about 100:1, the largest signal obtained to date.

The squid axon contains many structures and molecules that are aligned with respect to its long axis, including radially oriented components in the membrane (Schmitt & Bear, 1937; Cohen, Hille & Keynes, 1970). Since the electric field associated with the membrane potential is also radially oriented, it seemed possible that the dye molecules responsible for the optical signals would also be partially or completely aligned. If this were the case, then the absorption change with light polarized parallel to the long axis of the axon might differ from the absorption perpendicular to the long axis. The existence of such a dichroism would imply that there would also be a dye related birefringence signal. Both kinds of signals were found and their wavelength dependence was determined. These results, along with measurements of the wavelength dependence of the absorption and fluorescence changes, provide information that can help determine the mechanism(s) responsible for the optical signals.

One difficulty with the use of the merocyanine dye (Davila *et al.*, 1973) to monitor membrane potential was the photodynamic damage (Arvanitaki & Chalazonitis, 1961; Pooler, 1972) produced by intense light in the presence of oxygen. The damage found using this dye seriously limited experiments on invertebrate ganglia and on striated muscle (Salzberg *et al.*, 1973; Oetliker, Baylor & Chandler, 1975; Vergara & Bezanilla, 1976). In an effort to find less harmful dyes, we measured the photodynamic damage associated with each dye that had a relatively large signal. Several dyes with large signals were found that caused much less damage.

Preliminary reports of these experiments have been published (Ross *et al.*, 1974*b*; Ross, Salzberg, Cohen & Davila, 1974*a*; Ross *et al.*, 1975; Salzberg *et al.*, 1976), and several of our findings have since been confirmed (Tasaki & Warashina, 1975; Warashina & Tasaki, 1975; Tasaki, Warashina & Pant, 1976).

Materials and Methods

Giant axons with diameters of 300 to 750 μm were dissected from the hindmost stellar nerves of the squid, *Loligo pealii* and cleaned of small fibers. The apparatus used for simultaneous measurements of absorption and fluorescence in giant axons is shown schematically in Fig. 1. Some components were described previously (Cohen *et al.*, 1974). Light from a quartz-Halogen tungsten-filament lamp was passed through heat and interference filters (filter 1) and focussed onto a 5 mm spot centered on the axon. Barrier filters (filter 2) passed the emitted fluorescence and prevented scattered incident light from reaching the photodetector in the fluorescence measurement. For the absorption measurement, an image of the axon was formed with a microscope objective and a slit was positioned in the image plane parallel to the axis of the axon so that only light passing through the axon reached the detector. In some experiments the slit was narrowed so that the light reaching the detector was restricted to that passing through the edge or the center of the axon. The field of view of the objective lens restricted the absorption measurement to light passing through a 1.5 mm length of axon.

The light intensity reaching the photodetector in the absorption measurements was about 100 times larger than in the fluorescence measurements. An important source of noise in these measurements is the statistical fluctuation in the rate of arrival of photons at the photodetector (Braddick, 1960; Cohen, Hille & Keynes, 1969). Since this noise is proportional to the square root of the resting intensity, the ratio of this noise to the total light signal in absorption measurements was 10 times less than in fluorescence measurements. Unfortunately, the reduction in the contribution of the statistical noise revealed vibrational sources of noise that were difficult to eliminate entirely, even though the following steps were taken. The apparatus, from lamp housing to photodiode, was bolted to the Benelex top of a vibration isolation system having a 1.1 Hz resonant frequency (Lansing Research Corp., Ithaca, N.Y.). Low frequency vibration (less than 5 Hz) was often reduced after preventing the convection cooling of the lamp by blocking all the openings in the lamp housing. With these precautions, the vibrational noise was usually reduced to less than 10^{-5} of the resting intensity, but sometimes (e.g., the base-line drift in Fig. 10, top trace) this noise was significant.

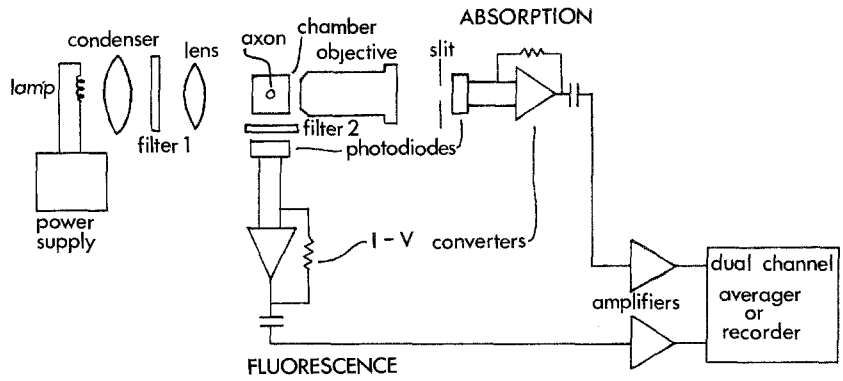

Fig. 1. Schematic diagram of the apparatus used for simultaneous measurements of absorption and fluorescence of a squid axon. Filter 1 was an interference filter whose width at half-height was 30 nm unless otherwise indicated. For wavelengths between 450 and 720 nm these filters were obtained from Oriel Optics Corp., Stamford, Conn. and Oriel G-766-7100 heat filters were placed between the condenser and filter 1. For longer wavelengths the interference filters were obtained from Karl Feuer Associates, Upper Montclair, N.J. These filters were blocked to 1.3 μ and Schott RGN9 glass (Schott Optical Glass, Inc., Duryea, Pa.) was used as the heat filter. The barrier filters (filter 2) were obtained from Schott Optical Glass, Inc. For the absorption measurements an image of the axon was formed with a Zeiss 10X, 0.22 N.A. objective lens, and slits in the image plane were used to block the light that did not pass through the axon. For measurements of absorption using polarized incident light, a Polaroid HN or HD polarizer was placed in the incident beam next to the chamber. For measurements of birefringence, a second polarizer, oriented at 90 ° to the plane of polarization of the first, was placed between the chamber and objective lens. In later experiments (Fig. 6*D* and Fig. 8) a calcite Glan-Thompson polarizer was used before the axon and the analyzer was a calcite Ahrens polarizer. The calcite polarizers (Karl Lambrecht Corp., Chicago) provided better extinction, especially at wavelengths longer than 850 nm. The photodetectors were SGD 444 manufactured by E.G. & G., Inc., Salem, Mass. The coupling capacitors, C, blocked the steady state and low-frequency components of the optical signal; to measure the resting intensity the capacitor was removed from the circuit. The coupling time constant was about ten times the sweep duration. The high frequency response time constants were limited to the values given in the figure legends by using the high frequency cut off on Tektronix 3A9 amplifiers. The optical response time constant was measured using a Monsanto MV-50 light-emitting diode to provide a step change in light intensity. The output of the 3A9 amplifier was either photographed or fed into a Data Laboratories Ltd. Biomac 1000 signal averager which was used either to record single trials or to average several sweeps.

Several components of the apparatus are strongly wavelength dependent; the output of the light source and the quantum efficiency of the photodetector both increase monotonically between 350 and 900 nm. In order to calculate the relative absorption and birefringence changes at different wavelengths and to determine the relative effectiveness of various excitation wavelengths while measuring fluorescence (Figs. 6, and 7), the observed changes in photodiode output were corrected for the efficiency of the apparatus as a function of wavelength. To correct the absorption spectra the photodiode output was measured for each incident light filter (filter 1) in the absence of an axon. The correction factor for each wavelength was simply 1/(diode output) and the experimental results were multiplied

by this factor. To obtain the correction factors for absorption of polarized light the same precedure was followed except that a single polarizer was inserted in the light path. For the birefringence spectra, two polarizers with parallel polarization were inserted into the light path. Since the excitation spectra for the fluorescence changes were determined with a fixed barrier filter (filter 2), the photodiode always measures light of the same spectral distribution unless the emission spectrum of the dye changes as a function of incident wavelength. The wavelength dependence of the fluorescence photodetector was not included in the correction factor for the excitation results. To obtain the correction factor for the excitation spectra, the correction factors for absorption spectra were divided by the quantum efficiency of the photodiode (determined from the manufacturer's specifications).

The electrodes and amplifiers used for voltage-clamp experiments were the same as previously described (Cohen, Keynes & Landowne, 1972; Davila *et al.*, 1974) and compensation for the resistance in series with the membrane was used (Davila *et al.*, 1974). Dyes added to the inside of the axon membrane were microinjected into the axoplasm using the technique of Hodgkin and Keynes (Keynes, 1963).

Axons were stained with several different concentrations of the dye in the range 0.01–1.0 mg/ml in an effort to find the concentration which gave the largest signal. After incubation with the dye for 10–20 min, the dye solution was usually replaced with sea water that had been bubbled with nitrogen or argon gas. The deoxygenation effectively eliminated any photodynamic damage to the axon. The preparation of the dye solutions has been described previously (Cohen *et al.*, 1974). Of the dyes in Table 2, 0.2% Pluronic F127 (a nonionic surfactant, BASF Wyandotte Corp., Wyandotte, Mich.) was used with dyes I, XVIII, XX, and XXI. All dye solutions were prepared just prior to the incubation since standing at room temperature often led to loss of color or to an increase in turbidity. With some dyes the color loss was pH sensitive and intense light often caused bleaching. The incubation of the axon was carried out at temperatures between 21 and 30 °C. In earlier experiments, lower temperatures were used but the procedure was changed when it was observed that the signal with dye XXI was larger if the incubation was carried out at higher temperatures. With most dyes the signal measured just after incubation was similar to that found following several exchanges of the sea water in the chamber over a period of 10–30 min. Except where specifically mentioned, all the experiments were carried out at room temperature, 21–23 °C.

The sources of the dyes used in these experiments are given in Table 1. The letters following the dye structure in Table 2 and the letters in parentheses in the Appendix refer to the letter and source in Table 1. Small samples of the dyes that we synthesized for these experiments (*H*) can be obtained by writing to Dr. A.S. Waggoner, Dept. of Chemistry, Amherst College, Amherst, Mass., 01002. The dyes labeled NK can be purchased from Nippon Kankoh-Shikiso Kenkyusho Co., Ltd., 2-3 Shimoishii 1 Chome, Okayama-Shi, Okayama, Japan. Synthetic procedures used for making two of the dyes labelled *H* are given below.

Synthetic Procedures

The dyes were synthesized according to general procedures described by Brooker *et al.* (1956). Some description was given previously (Cohen *et al.*, 1974). All dyes decomposed upon melting. When chromatographed on Eastman Chromagram silica gel thin-layer sheets with a variety of solvent systems, each dye showed a single visible spot. Iodine staining revealed no additional spots. The synthetic procedures for dyes XVII and XXI are described below as examples.

5-[(1-γ-Triethylammonium sulfopropyl-4(1H)-quinolylidene)-2-butenylidene]-3-ethylrhodanine (XVII). A mixture of 5-(γ-acetanilidoallylidene)-3-ethylrhodanine (3.3 g, 10 mmole)

Table 1. Dye sources

B.	Fisher Scientific Co.
C.	MC & B Manufacturing Chemists
D.	Allied Chemical Corp.
F.	K. & K. Laboratories, Inc.
G.	Eastman Research Laboratories
H.	synthesized for these experiments
K.	Calbiochem
L.	Aldrich Chemical Co., Inc.
M.	Eastman Kodak, Co.
N.	L.B. Holliday & Co., Ltd.
Z.	Polaroid Corp.
AA.	Minnesota Mining and Manufacturing Co.
NK.	Nippon Kankoh Shikiso Kenkyusho Co., Ltd.
PD.	Parke, Davis & Company
XE.	Xerox Corp.
IL.	Ilford Ltd.
CG.	Ciba Geigy Corporation
GA	GAF Corp.
JH.	Dr. Jack W. Hauser
SL.	Dr. Solomon V. Levin

and anhydro-1-γ-sulfopropyllepidine hydroxide (2.6 g, 10 mmole) in a solution containing 25 ml of methanol, 25 ml of DMF and 5 ml of triethylamine was refluxed for 45 min. After cooling 50 ml of ether was added. The solution was decanted to a 500 ml flask, and 400 ml of ether was added to the flask. The flask was placed in a refrigerator overnight. The crystals were collected and rinsed well with ether, yielding 1 g of greenish brown crystals, mp 185–188 ° (softens at 160 °C). Attempts to further recrystalize the dye from various solvent systems always caused considerable decomposition. The absorption spectrum of the dye, XVII, in ethanol showed two broad peaks with maxima at 662 and 716 nm.

Bis-[1,3-dibutylbarbituric acid-(5)]-pentamethine oxonol (XXI). A mixture of 1,3-dibutylbarbituric acid (2.4 g, 10 mmole) and glutaconaldehyde dianilide hydrochloride (1.4 g, 5 mmole) in 30 ml of absolute ethanol and 5 ml of triethylamine was refluxed for 30 min and poured into 300 ml of dilute HCl. The crude dye was collected after chilling and recrystalized several times from aqueous ethanol, yielding 1.5 g of final product. In some runs recrystalization failed to give a clean product, so final purification was done by using a silica gel column. The column was eluted first with a benzene-acetone (50:50) mixture; the proportion of acetone was gradually increased. The pure dye melts at 305–308 °C (softens at 260 °C) and has an absorption maximum in ethanol at 590 nm.

Results

Absorption

With the apparatus diagramed in Fig. 1 the light power reaching the photodetector was 2.9×10^{-4} W (8×10^{8} photons/μsec) in an experi-

ment with a 500 μm diameter axon and filter 1 with a peak transmission of 750 nm. After the axon had been incubated for 10 min with 0.2 mg/ml of a merocyanine-rhodanine dye (XVII)[1], the power decreased to 2.4×10^{-4} W. When the axon was stimulated to make an action potential, the light intensity reaching the detector changed by a small amount with a time course nearly identical to that of the action potential (Fig. 2).

Controls. Several experiments described below showed that the intensity increase in Fig. 2 was due to a decrease in absorption and not the result of an artifact or the result of interference from a change in light scattering or fluorescence. No signal was found when the light was off, eliminating the possibility that the intensity change resulted from electrical coupling between the light and electrical measuring systems. Although there are changes in intrinsic light scattering that accompany the action potential (Cohen *et al.*, 1972), they are not the source of the changes shown in Fig. 2. The intrinsic changes had signal-to-noise ratios about 500 times smaller than the absorption signal and furthermore, in voltage clamp experiments, the time course of the absorption change was qualitatively different from the time course of the scattering change. In one experiment, carried out with dye I, a second filter, identical to filter 1, was placed between the chamber and objective lens. This second filter prevented fluorescent light from reaching the absorption photodetector but did not affect the fractional intensity change measured by that photodetector. Therefore the signal in Fig. 2 could not be the result of a change in fluorescence emitted in the direction of the incident beam. (The emitted light reaching the absorption photodetector was about 1,000 times less intense than the transmitted light and thus a fractional change in fluorescence of 10^{-3} would result in a fractional change in transmission of only 10^{-6}, two orders of magnitude smaller than the observed changes in transmission.) Finally, the wave-length dependence of the intensity changes measured with the absorption photodetector (*see* below) would be very difficult to explain as an artifact or interference from other optical signals. We conclude that the intensity increase shown in Fig. 2 actually resulted from a decrease in absorption by the dye-stained axon.

The absorption change had a time course very similar to the time course of the potential change, suggesting that absorption was sensitive to changes in membrane potential and not sensitive to the ionic currents

[1] Roman numerals refer to dyes in Table 2 of this paper and Tables 3 and 4 of Cohen *et al.* (1974); Arabic numerals refer to dyes listed in the Appendices of the two papers.

or the membrane conductance increases that occur during the action potential. This suggestion was tested (*see* Davila *et al.*, 1974) by measuring absorption during voltage clamp steps. An experiment using dye XVII is shown in Fig. 3. During the hyperpolarizing step (middle trace, on the left) the ionic currents (bottom trace) were very small and there were no conductance changes (Hodgkin & Huxley, 1952), but there was a change in absorption (top trace) that had a time course similar to the change in potential. Since the currents were small and there was no change in conductance, it is likely that this absorption signal was related to the change in potential. Furthermore, during the depolarizing step, on the right, there were large increases in conductance accompanied by large ionic currents, but the absorption signal again had the same shape as the change in membrane potential. When four potential steps were used and the size of the absorption change was plotted against the size of the potential step, the results in Fig. 4*A* were obtained. The absorption signal of dye XVII was linearly related to membrane potential over the range ± 100 mV from the resting potential.

Signal Size

Because voltage-clamp experiments similar to the one illustrated in Fig. 3 were convenient and provided preliminary information about the mechanism and time course of the optical signal, they were used routinely in our efforts to find larger signals. In these experiments both absorption and fluorescence were measured. Using the procedures in Cohen *et al.* (1974), we calculated the signal-to-noise ratio during a single 50 mV depolarizing step. The results obtained with several dyes which gave relatively large changes are given in the last column of Table 2; results with additional dyes are given in the Appendix. Many of the signal-to-noise ratios in Table 2 are larger than any achieved previously (Cohen

Fig. 2. Changes in absorption (dots) of a giant axon stained with dye XVII during a membrane action potential (smooth trace) recorded simultaneously. The change in absorption and the action potential had the same time course. In this and subsequent figures where the original absorption measurements are shown, the direction of the vertical arrow to the right of the trace indicates the direction of an increase in absorption; the size of the arrow represents the stated value of a change in absorption, ΔA, in a single sweep divided by the resting absorption due to the dye, A_r. All records are traced from photographs of the Biomac cathode ray tube or from *x-y* recordings. Filter 1 had a peak transmission of 750 nm; 32 sweeps were averaged. The response time constant of the light measuring system was 5 μsec

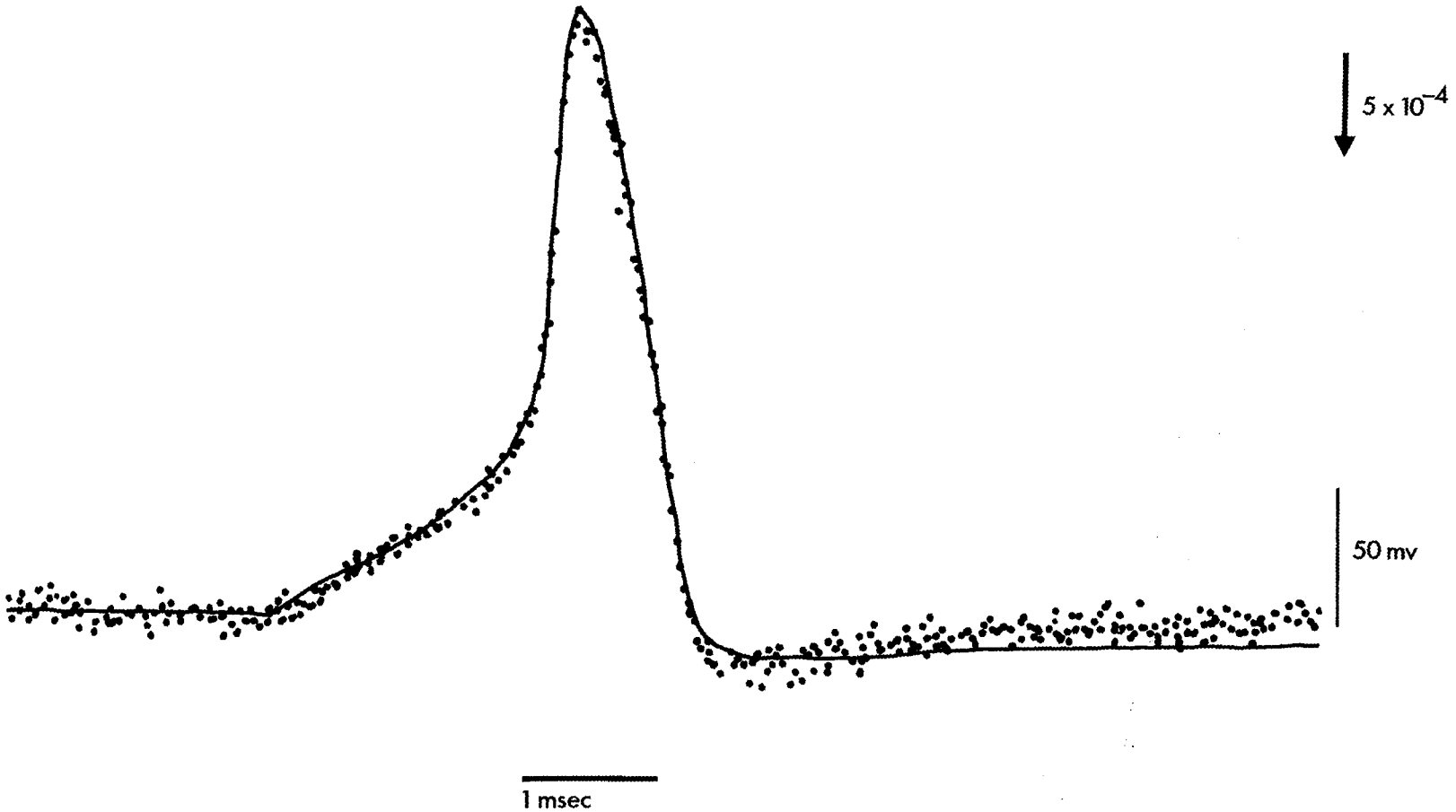

Fig. 2

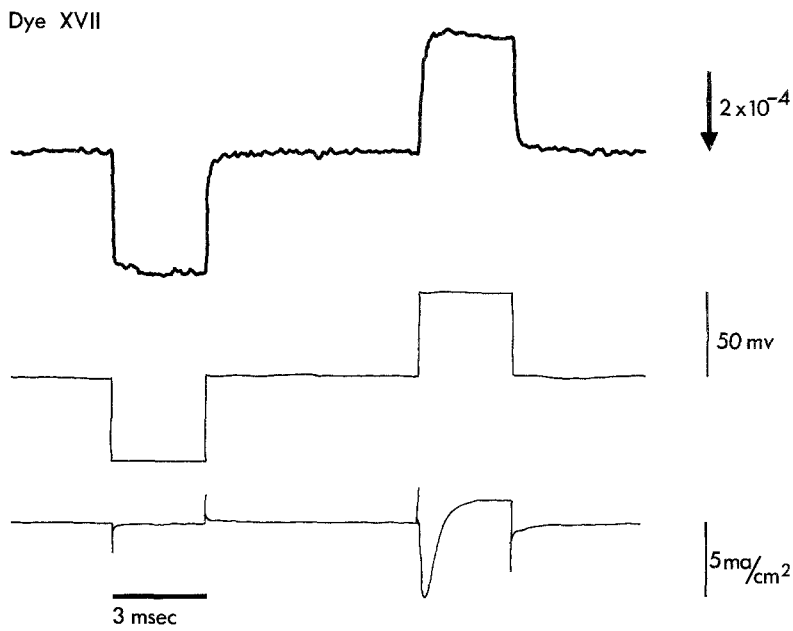

Fig. 3. Changes in absorption of an axon stained with dye XVII (top trace) during hyperpolarizing and depolarizing potential steps (middle trace). The bottom trace is the current density. The absorption changes had the same shape as the potential changes and were insensitive to the large currents and conductance changes that occurred during the depolarizing step. In this and subsequent figures the holding potential was the resting potential, and hyperpolarization is represented downward; inward currents are downward. Filter 1 had a peak transmission at 750 nm; 128 sweeps were averaged; the time constant of the light measuring system was 20 μsec. The axon was stained in a 0.01 mg/ml solution of the dye

et al., 1974) even though the efficiency of the apparatus was identical. The signal-to-noise ratio varied somewhat from axon to axon. For example, in experiments on 10 axons the range of signal-to-noise ratios in fluorescence measurements with the merocyanine dye, I, was between 1 and 10; in absorption measurements on 10 axons using the merocyanine-rhodanine dye, XVII, the range was between 20 and 40.

While the signal-to-noise ratio provides a good indication of which dyes are likely to be useful for monitoring membrane potential, its value is dependent on the apparatus used in the measurement (*see* discussion on page 10 of Cohen *et al.*, 1974). For example, in our apparatus the overall efficiency at 375 nm is about 50 times less than the efficiency at 660 nm, so that the signal-to-noise ratio at 375 nm is about 7 times smaller than that at 660 for the same fractional change (when statistical fluctuations in the rate of arrival of photons at the photodetector is the predominant source of noise). On the other hand, the fractional

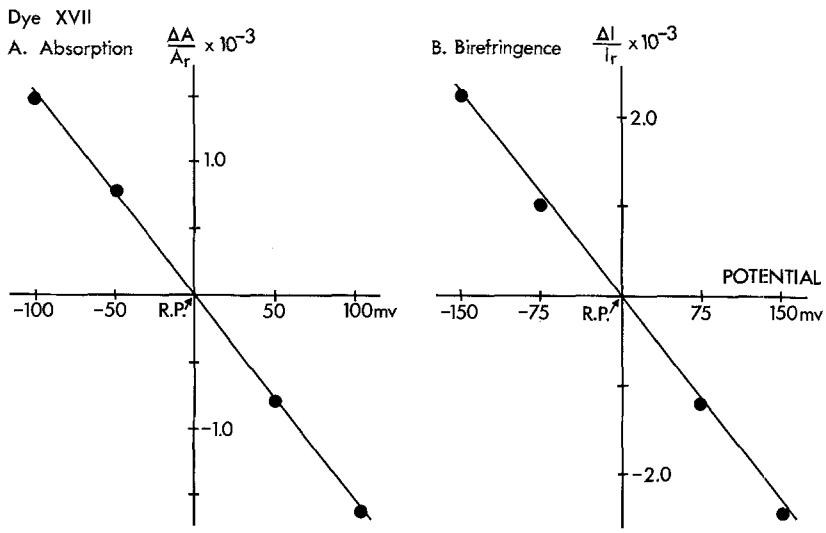

Fig. 4. Change in dye XVII absorption (*A*) and birefringence (*B*) as a function of membrane potential. Both the absorption and birefringence of dye XVII were linearly related to membrane potential over the range tested. The ordinate in the birefringence measurement was the change in intensity divided by the total intensity resulting from intrinsic and extrinsic birefringence. The axon was stained in a 0.4 mg/ml solution of the dye. Filter 1 had a peak transmission of 750 nm for both experiments. Other dyes whose absorption, fluorescence, and birefringence changes were linearly related to membrane potential were dyes I (A,F and B),XVIII (A), XIX (A and F), and XX (A,F and B). For dyes 313 and 433 two straight lines seemed best to fit the relationship between the absorption and potential (*see* Fig. 5*A* of Cohen *et al.*, 1974). The fast phase of the fluorescence change of dye XXI was linearly related to membrane potential while the slow component with this dye and the fluorescence change of dyes 313 and 417 were related to potential in a more complicated fashion

change in absorption or fluorescence is more independent of the experimental apparatus and these values for a 50 mV depolarization are also given for the dyes in Table 2. $\Delta F/F_r$ is the change in fluorescence intensity divided by the resting fluorescence intensity due to the dye, while $\Delta A/A_r$ is the change in transmitted intensity divided by the reduction in resting transmission due to staining by the dye. $\Delta A/A_r$ is equal to $-\Delta T/(T_{r,\text{before}} - T_{r,\text{ after staining}})$. (*Note:* This definition of the absorption change should not be confused with the absorbance change defined elsewhere [Waggoner *et al.*, 1976]). The wavelength of incident light at which the largest signal-to-noise ratio was found is also given in Table 2.

Photodynamic Damage

A difficulty sometimes associated with use of dyes to monitor membrane potential has been the photodynamic damage caused by intense

Table 2. Dyes with relatively large changes in absorption or fluorescence.[a]

		Source	Wavelength (nm)	Mode	$\Delta F / F_r$ or $\Delta A / A_r$	S/N
I	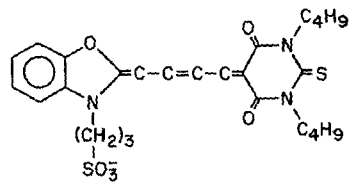	M	570	abs. fluor.	$+5 \times 10^{-4}$ $+10^{-3}$	10 5
XVII	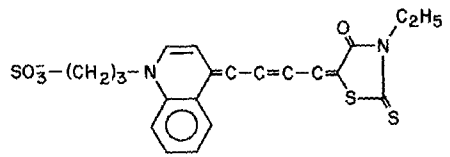	H	750	abs.	-5×10^{-4}	30
XVIII	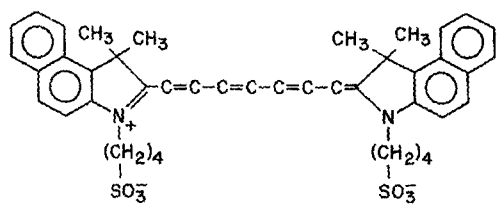	M	840	abs.	-10^{-4}	10

XIX	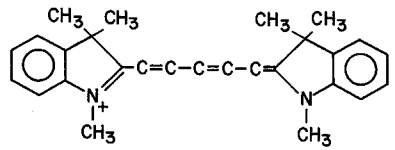	H, NK	660	abs. fluor.	$+10^{-5}$ $+10^{-4}$	2 2
XX	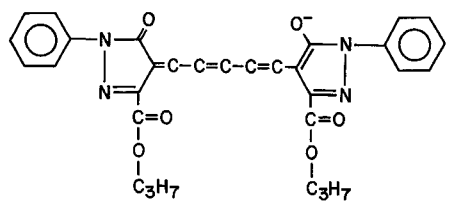	Z	690	abs.	$+5 \times 10^{-5}$	10
XXI	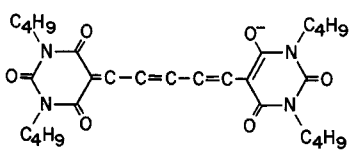	H	600	fluor.	$+10^{-3}$	15

[a] When both signals were large, both are given; when only one of the signals was large, data about the other was omitted. For dye XVIII fluorescence was not measured.

light in the presence of oxygen. For example, in experiments carried out in aerated sea water, when an axon stained with dye I was illuminated with an intensity of 0.1 W/cm^2 the sodium current was reduced by 50% after only 9 sec. Because this damage can cause serious difficulty where it would be unphysiological or difficult to remove the oxygen, we have looked for dyes that are less damaging. The results for eleven dyes giving large signals are shown in Fig. 5. The three merocyanine-thiobarbital dyes (I, IX and 403) caused the most rapid damage, while cyanines (366, XIX, XVIII), oxonols (489, XX, XXI) and merocyanine-rhodanines (XVII and 433) all led to damage that occurred at least an order of magnitude more slowly. The rate of reduction of sodium current using dye XVII was less than three times faster than the rate in the absence of dye. In addition, in experiments with dye XVII on leech segmental ganglia (B.M. Salzberg and L.B. Cohen, *unpublished results*) and on frog muscle (S.M. Baylor, W.K. Chandler and D.T. Campbell, *personal communication*) no photodynamic damage could be detected although there were large potential-related signals. Thus, the damage caused by photodynamic effects can be reduced to insignificant levels by an appropriate choice of dye.

At the concentrations used for experiments reported in Fig. 5 or Table 2 none of the dyes caused appreciable changes in ionic currents in the absence of light. In one experiment, synaptic transmission between a pressure cell and an L motoneuron in a leech segmental ganglion was found to be unaffected by incubation in a Ringer's containing dye I. In addition, incubation of day old squid in a 0.1 mg/ml solution of dye XVII for 60 min had little effect on their activity although staining was evident.

Wavelength Dependence of Absorption

The change in absorption of an axon stained with the merocyanine-rhodanine dye, XVII, (Figs. 2 and 3) was largest for light of 750 nm, but absorption changes were also found at other wavelengths. The change in intensity transmitted by the stained axon during a 50 mV depolarizing step was corrected for the efficiency of the apparatus as a function of wavelength to give a corrected absorption change. This value is plotted as a function of wavelength in Fig. 6*A*. At all wavelengths between 450 nm and 890 nm there was a decrease in absorption during a depolarization.

Absorption changes that were in one direction at all wavelengths were obtained with only a few dyes in addition to dye XVII and all

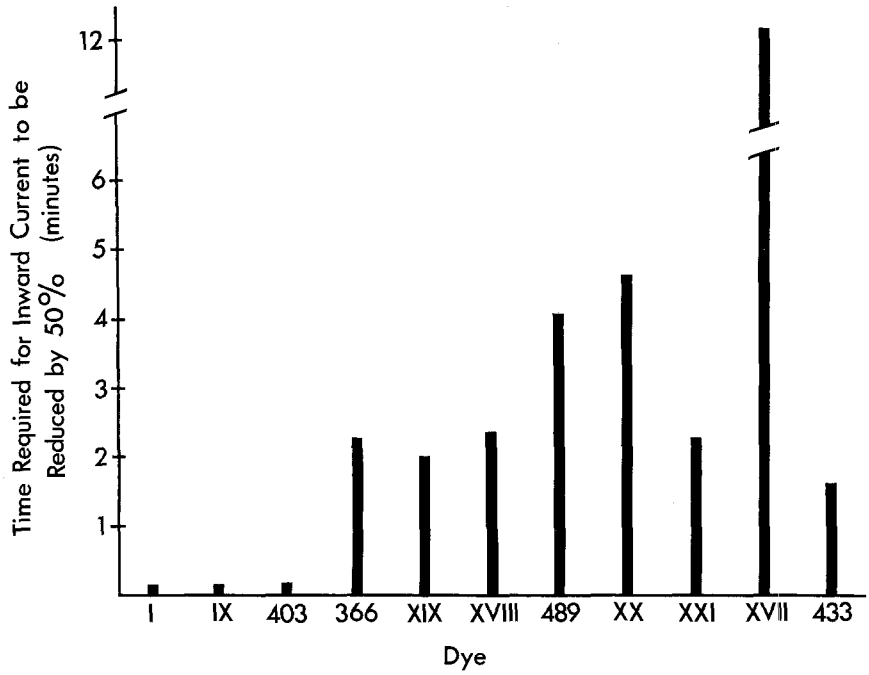

Fig. 5. The time required for a 50% reduction in inward current after turning on light in aerated sea water. The light intensity and wavelength were identical to those used in the experiments to measure signal-to-noise ratios. Dyes I, IX and 403 (thiobarbital merocyanines) caused rapid damage, while the other dyes led to much slower deterioration in the current. Depolarizing voltage clamp steps were imposed on the axon at the rate of 10/sec during the measurement. When no dye was present it took approximately 40 min for the inward currents to decline to 50%. In the presence of dye I the removal of oxygen from the sea water also resulted in survival times of minutes. For some dyes the measurement was made only once; where several measurements were made the mean time (shown in this figure) was usually within a factor of two of the fastest and slowest times

were analogues of dye XVII. With most dyes the sign of the absorption change was different at different wavelengths. The relative absorption change of the merocyanine dye, I, as a function of wavelength is shown in Fig. 7*A*. During a depolarizing step there was a decrease in absorption between 450 and 540 nm and an increase between 550 and 600 nm. In addition there was a small decrease found between 610 and 640 nm which was overlooked in our preliminary experiments (Ross *et al.*, 1974), and not found by Tasaki *et al.* (1976). We feel that the small decrease at long wavelengths provides important limitations on the possible molecular mechanisms responsible for the signal (*see* Discussion). Later experiments showed that the spectra of ΔA *vs.* wavelength depends on the concentration of the dye in the staining solution (L.B. Cohen, A. Grin-

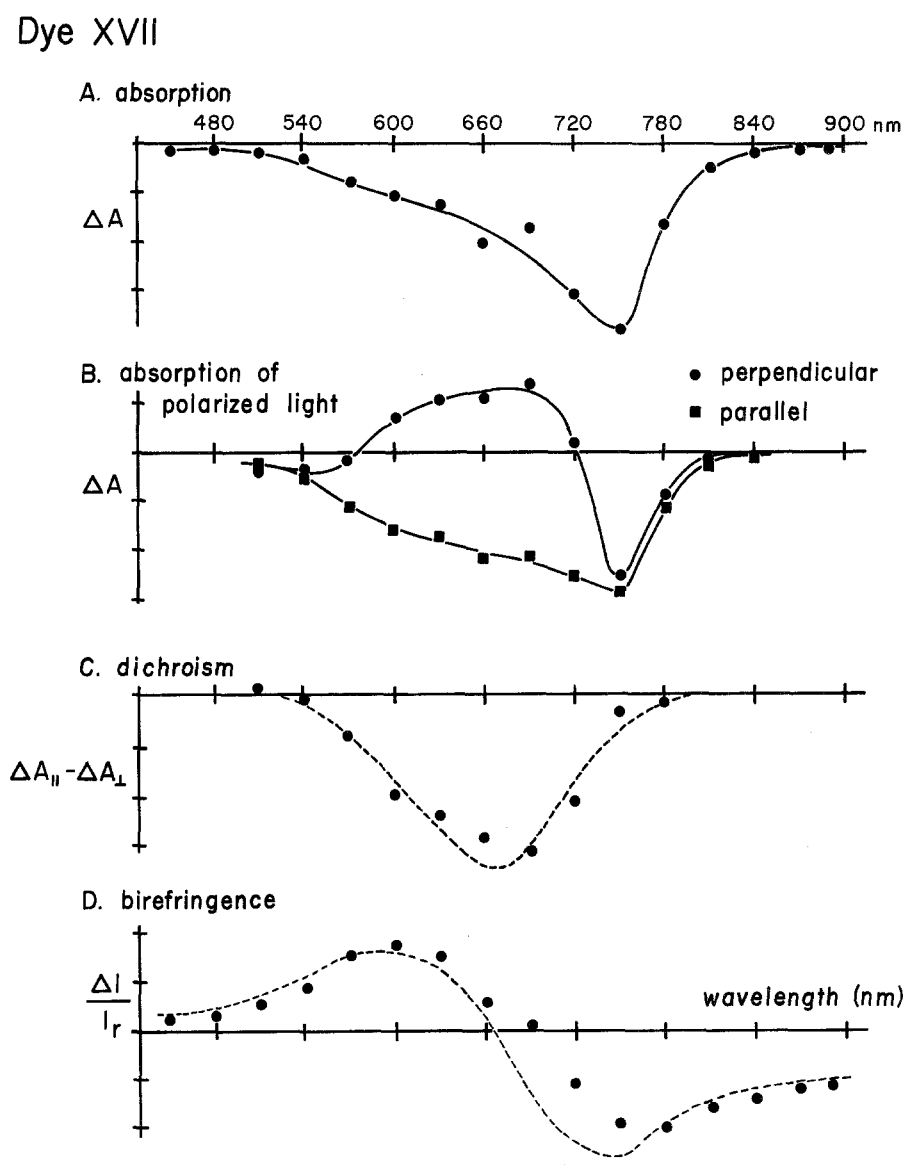

Fig. 6. The wavelength dependence of the changes in absorption of unpolarized light (*A*), of the changes in absorption of polarized light (*B*), of the dichroism (*C*), and of the birefringence (*D*), all measured during 50 mV depolarizing steps on axons stained with dye XVII. The peak transmission of the interference filters (filter 1) is shown on the abscissa. The ordinates for *A-C* are the changes in absorption ΔA, corrected for the efficiency of the apparatus. The ordinate for *D* is the change in intensity (stained axon) divided by the resting intensity (unstained axon) when the axon is between perpendicular polarizers at 45 °. (*A*). At all wavelengths measured the absorption of dye XVII decreased during a depolarization. Other dyes whose absorption changes were in the same direction at all wavelengths measured were 433, 173, and 458. (*B*). The absorption change of dye XVII was very dependent upon the plane of polarization of the incident light. For light

vald, K. Kamino, B.M. Salzberg, *unpublished results*). With several other dyes (*see* legend of Fig. 7) the spectra of the absorption signals were measured carefully enough and results like that found for dye I were obtained; the absorption spectra were triphasic with a small inversion at long wavelengths.

Dichroism

Changes in absorption using light polarized either parallel or perpendicular to the axis of the axon were measured to determine whether the absorption signal is dichroic. The results of such an experiment, for an axon stained with dye XVII, are shown in Fig. 6*B*; a large dichroism is obvious. In fact, at some wavelengths the sign of the absorption change is opposite for the two directions of polarization. At other wavelengths, 480 to 540 nm and 750 to 840 nm, the absorption change exhibits relatively little dichroism. (In one experiment we measured absorption changes for both polarized and unpolarized light on the same axon, and, as expected, the sum of the absorption signals measured with the two orthogonal planes of polarization equalled the absorption signal with unpolarized light. This relationship is not exactly preserved in Fig. 6 where the experiments in *A* and *B* were carried out on different axons.) When dichroism measurements were carried out with dye I, the dichroism was smaller but it occurred at all wavelengths where an absorption signal could be measured (Fig. 7*B*).

Birefringence

A measurement of linear dichroism is related to a measurement of birefringence in the same sense that circular dichroism and optical rotation (circular birefringence) are equivalent and absorption and refractive

polarized parallel to the long axis of the axon (filled circles) there was a decrease in absorption at all wavelengths while for light polarized perpendicular to the long axis (open circles) there was an increase in absorption between 600 nm and 690 nm. (*C*). The absorption changes in *B* were subtracted to give the dichroism. The experimental points are shown as filled circles. The dashed curve is the fitted sum of two Gaussian curves. (*D*). The experimental points are fit reasonably well by the theoretical curve derived from the dichroism spectrum using a Kramers-Kronig transformation (Houssier & Kuball, 1971). The absorption (*A*) and birefringence spectra (*D*) were recorded on the same axon; the absorption of polarized light (*B*) was measured on a second axon; both axons were stained in 0.2 mg/ml solutions of the dye. The solid curves connecting the experimental points in parts *A* and *B* were drawn arbitrarily

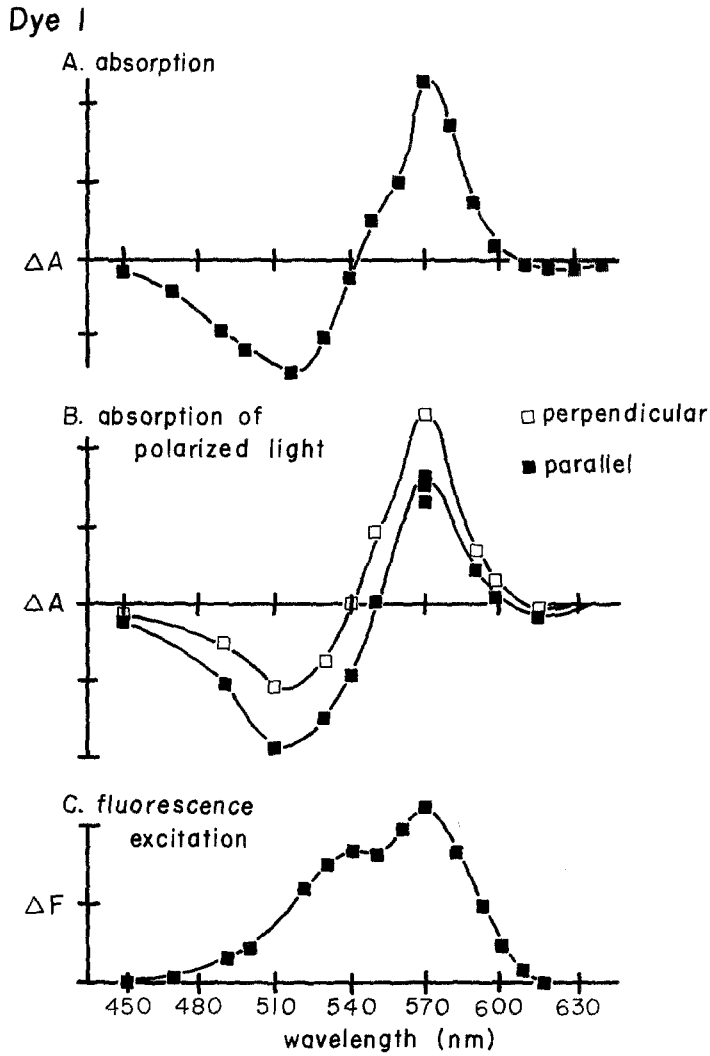

Fig. 7. The wavelength dependence of the changes in absorption of unpolarized light (*A*), of the change in absorption of polarized light (*B*), and the size of the fluorescence change as a function of incident wavelength (*C*) measured during 50 mV depolarizing steps on axons stained with dye I. The peak transmission of the interference filters (10 nm width at half-height, filter 1) is shown on the abscissa. The ordinates in (*A*), (*B*), and (*C*) are the intensity changes in absorption and fluorescence measurements corrected for the efficiency of the apparatus. (*A*). The direction of the absorption change was wavelength dependent, reversing sign twice. There were absorption increases at wavelengths between 550 and 600 nm, and absorption decreases between 450 and 530 nm and between 610 and 640 nm. Similar small reversals at long-wavelengths, in addition to the more prominent reversal, were found with dyes XX, XXI, 412, 305, 489, and 397. With several other dyes, XIX, 13, 366, 138, 403, 405, 448, 329, and 318, less careful measurements were made, but prominent reversals in sign as a function of wave-length were found. (*B*). The

index are equivalent (Houssier & Kuball, 1971; Fredericq & Houssier, 1973). Thus, from the dichroism demonstrated for the absorption signals of dyes XVII and I (Figs. 6*B* and 7*B*), one would predict changes in extrinsic birefringence in addition to the intrinsic birefringence changes described previously (Cohen *et al.*, 1970, 1971). Therefore, crossed polarizers oriented at 45 ° to the long axis of the axon were positioned on either side of the chamber and changes in the transmitted intensity at 810 nm were measured during voltage clamp steps. In an unstained axon the intensity changes were relatively small (Fig. 8, top trace). (Additional averaging provided clear evidence of the intrinsic signal which was, expectedly, larger during hyperpolarizing steps than during depolarizing steps.) Following a 15-min incubation with dye XVII, the signal (Fig. 8, second trace) was more than an order of magnitude larger than the intrinsic signal and, unlike the intrinsic signal it was linearly proportional to membrane potential over the range ± 150 mV from the resting potential (Fig. 4*B*). While incubation with the dye caused a dramatic increase in the intensity change induced by a potential step, the change in resting intensity was small at all wavelengths. In the experiment illustrated on the top two traces of Fig. 8, the intensity reaching the photodetector with the unstained axon was 10^{-5} W and incubation with a 0.2 mg/ml solution of dye XVII changed this by less than 25%. Accordingly, the fractional change in intensity, $\Delta I/I_r$, where I_r is the change in resting intensity due to the dye, was relatively large, almost 10^{-2}.

Two kinds of experiments indicated that the extrinsic signal shown in Fig. 8, second trace, was the result of a change in optical retardation. (Retardation is the product of birefringence and path length.) When the angle between the axons's axis and the plane of polarization of the incident light was changed from 45 ° to 90 °, no signal was measured. This observation suggests that the signal found at 45 ° resulted either from a change in optical retardation or a change in linear dichroism,

absorption signals, measured at the edge (using a slit in the image plane 1/4th the diameter of the axon) with light polarized parallel to the long axis of the axon (filled circles) or light perpendicular to the long axis (open circles). At all wavelengths the signals were different for the two polarizations although the differences were not as large as those obtained for dye XVII. The dichroism was sometimes difficult to demonstrate if light from the entire axon was measured. (*C*). At all excitation wave-lengths the fluorescence emission at wavelengths longer than 630 nm increased during a depolarization. The absorption (*A*) and excitation (*C*) spectra were from simultaneous measurements on an axon that had been stained with a 0.2 mg/ml solution of the dye; the absorption of polarized light (*B*) was measured on a second axon stained with a 0.05 mg/ml solution. The solid curves connecting the experimental points were drawn arbitrarily

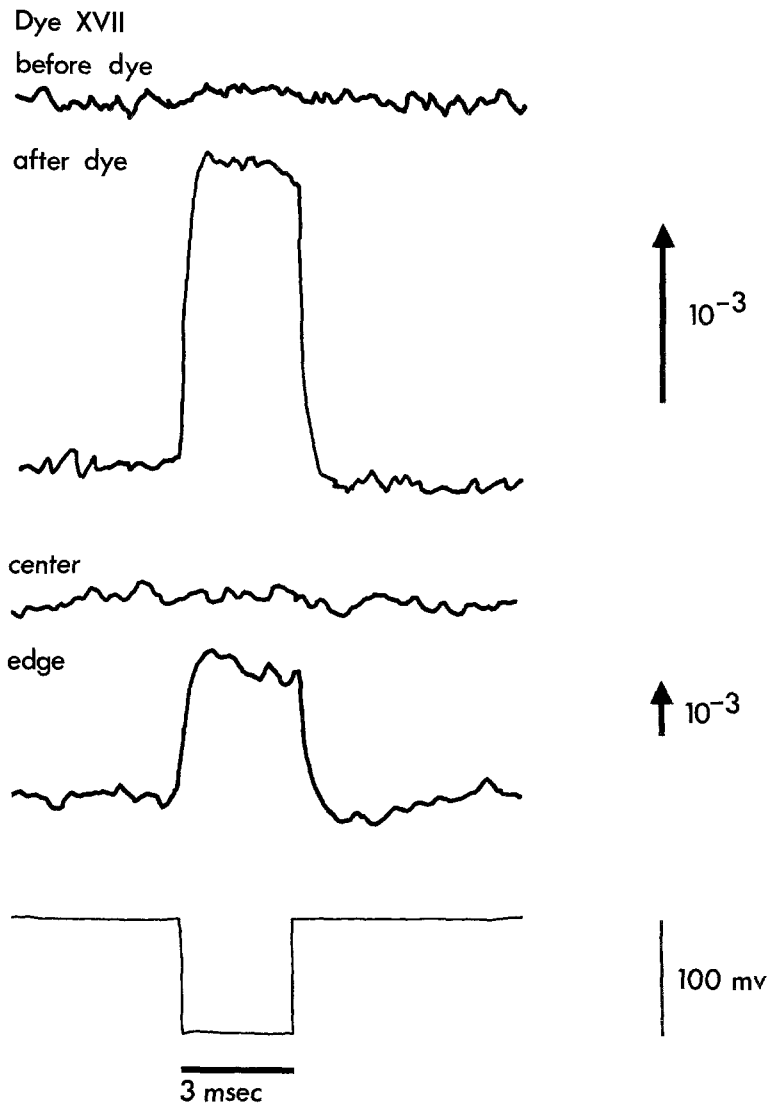

Fig. 8. Changes in light intensity during a 100 mV hyperpolarizing potential step (bottom trace) when an axon stained with dye XVII was placed between perpendicular polarizers and the axes of polarization were at 45 ° to the long axis of the axon. Before the axon was stained there was a small intrinsic signal which is difficult to discern in the top trace; after incubation with dye XVII the result in the second trace was obtained. With a narrow slit in the image plane positioned at the center of the axon's image (third trace) no signal was found; a relatively large signal was obtained when the slit was positioned at the edge (fourth trace), consistent with a radial optic axis for the birefringence signal. The direction of the vertical arrow to the right of the trace represents an increase in intensity; its size represents the stated value of the change in intensity divided by the resting intensity due to the axon. This resting intensity was the sum of that resulting from intrinsic and extrinsic birefringence. The top arrow applies for the top two traces; the bottom arrow applies for the bottom two. The interference filter (filter 1) had a peak

and it argues against possible contributions from light scattering, optical rotation or absorption. In a second kind of experiment using the quarter wave plate compensation method of de Senarmont-Friedel (Bennett, 1950), we found that when the resting retardation of the stained axon was compensated by rotating the analyzer, the intensity change was reduced by more than 90%. (Even though the signal was reduced by more than 90%, the resting intensity was reduced by only 70% at full compensation, an indication that the resting retardation was not quite uniform across the axon (Cohen *et al.*, 1970). With additional compensation the signal was reversed in direction but had the same time course. These results were obtained at 570, 750 and 900 nm, wavelengths where the dichroism is small. Thus, at these wavelengths, the signal measured with the axon between perpendicular polarizers resulted primarily from a change in optical retardation. We have no evidence to show whether the retardation signal results from a change in birefringence or path length but a dye related change in path length that depends on potential seems unlikely so we refer to this signal as a birefringence change.

When a similar compensation experiment was carried out at 690 nm, at the peak of the dichroism, the signal was only slightly altered when the resting retardation was fully compensated. We suppose that this results from the fact that at wavelengths where the absorption change is dichroic the signal found with the axon between perpendicular polarizers is the sum of intensity changes resulting from alterations in both optical retardation and dichroism (Houssier & Kuball, 1971).

The size of the signal found between perpendicular polarizers was measured as a function of wavelength for dye XVII and the changes in intensity found in a stained axon, divided by the resting intensity measured in an unstained axon, are plotted in Figs. 6*D*. Note that the signal occurs at wavelengths outside the absorption band of the dyes. The same kind of experiments were carried out with dye I over a narrower wavelength range. The relationship of the birefringence and dichroism spectra for dye I was similar to that shown in Fig. 6 for dye XVII.

The birefringence spectrum should be predictable from the dichroism spectrum. To make this calculation the absorption changes for light polarized parallel and perpendicular to the axon's axis in Fig. 6*B* were

transmission at 810 nm. The response time constant of the light measuring system was 170 μsec, 16 sweeps were averaged for the top two traces, 1024 sweeps for the bottom two. The experiment in the top two traces was carried out on one axon, a second axon was used for the experiment shown in the bottom traces; both axons were stained with a 0.2 mg/ml solution of the dye

subtracted to give the experimental dichroism spectrum shown in Fig. 6*C*. These experimental results were fitted to the sum of two Gaussians (dashed curve) and then transformed, using the Kramers-Kronig relation, into birefringence spectra (Δn, in arbitrary units) according to the method given by Houssier and Kubal (1971). The calculated birefringence spectrum was then converted to $\Delta I/I_r$ using Eq. (1):

$$\frac{\Delta I}{I_r} = \frac{k \Delta n}{\lambda} \cot \frac{1}{2} \left(\frac{2 \pi R}{\lambda} \right) \tag{1}$$

where k is a constant, R the retardation and λ the wavelength. Eq. (1) is derived from Eqs. (1) and (4) of Cohen *et al.* (1970). R was determined from a measurement of resting intensity at each wavelength and Eq. (3) of Cohen *et al.* (1970) using a calibration at 570 nm with a quarter-wave plate compensator and the efficiency of the apparatus as a function of wavelength.

The predicted curve for $\Delta I/I_r$, shown as the dashed curve in Fig. 6*D*, falls reasonably close to the experimental results. A better fit to the dichroism spectra using a sum of four Gaussians did not improve the agreement between the predicted and observed birefringence spectra. There are two kinds of deviations: the curve and experimental results clearly differ at the wavelengths where the absorption is dichroic, but this difference is approximately the one expected since the signal at those wavelengths includes components due to dichroism (*compare* Fig. 6*D* with Fig. 5 of Houssier and Kubal [1971]). In addition, even at wavelengths outside the dichroism band, the predicted curve and experimental points do not coincide exactly. This may result from additional dichroic bands in the ultraviolet which contribute to the birefringence changes in the visible, or there may be experimental errors (including relatively large errors in the experimentally determined dichroism, and somewhat smaller uncertainty in the resting retardation and the birefringence spectra, together with the circumstance that these data were obtained on three separate axons).

In addition to dye XVII, birefringence experiments were carried out with four other dyes. With the merocyanine dye, I, the cyanine dye, XVIII, and the oxonol, XXI, the largest signal-to-noise ratio was about the same size as that found with dye XVII while, with the cyanine dye, XIX, the signal was smaller.

Optic axis. By comparing the change in birefringence measured with light passing through the edge and the center of the axon, it was concluded

(Cohen, *et al.*, 1970) that the intrinsic birefringence change had a radial optic axis. To do similar experiments with the dye related signals we reduced the numerical aperture of the objective (in the direction perpendicular to the axon's axis) to 0.14 and narrowed the slit in the image plane (parallel to the axis) to 0.18 of the axon's diameter. These steps reduced the measured light to a narrow, nearly parallel beam passing through only a part of the axon. When the slit was positioned at the edge of the axon the large birefringence signal in the fourth trace of Fig. 8 was obtained; when the slit was at the center of the axon no signal was found (third trace). Careful measurements showed that for both dye XVII and dye I the signals at the center were at least 20 times smaller than the signals at the edge. Although 2.3 times more membrane area is imaged when the slit is at the edge than when it is at the center, the fact that the signal at the center is at least 20 times smaller shows that this geometrical consideration is not the dominant factor. Similarly, when the dichroism in the absorption signals were compared at the edge and the center, for both dye XVII and dye I the dichroism was much less marked at the center than at the edge. If the optical signal had a radial optic axis, then for light passing through the center of the axon the components of the absorption transition moment[2] parallel to the radial optic axis would be perpendicular to the electric vector of the incident light and the components perpendicular to the radial axis are randomly distributed, and therefore equal for all planes of polarization. Thus the dichroism and birefringence signals would vanish at the center. The experimental results are therefore consistent with the assumption that the dichroism and birefringence signals have a radial optic axis.

Fluorescence

Fluorescence experiments were carried out for each dye using the apparatus in Fig. 1 which, for fluorescence, was essentially identical to that described earlier (Cohen *et al.*, 1974). The results presented in Table 2 and Fig. 5 show that on squid axons a barbituric acid-oxonol (XXI) had a larger signal and was less damaging than was the merocyanine dye (I). The excitation spectrum of the fluorescence change of dye I was measured in several axons and the results of one experiment are shown in Fig. 7*C*. Later experiments showed that the shape of the

[2] When the transition moment of a molecule is parallel to the electric vector of the incident light the probability of absorption is highest.

spectrum depended on both the concentration of dye in the staining solution and on the wavelength at which the fluorescence emission was measured (L.B. Cohen, A. Grinvald, K. Kamino, and B.M. Salzberg, *unpublished results*).

Extrinsic Scattering

The finding that there is a substantial change in fluorescence with dye I, using an incident wavelength of 540 nm where the absorption signal is small, suggests that the changes in fluorescence result from changes in quantum yield or orientation of the dye molecules; the fluorescence changes are not solely the simple consequence of the changes in absorption. However, since there are changes in absorption, the light scattered by the axon will change as a direct result of the altered transmission. Indeed, in the absence of a barrier filter there was an intensity decrease during a hyperpolarizing step in an axon stained with dye XVII and its time course was similar to the absorption change. The fractional change in intensity was found to be equal to the fractional change in transmission; therefore, we concluded that this scattering change was a direct result of the change in absorption. (Dye XVII is only slightly fluorescent and the fluorescence change with barrier filters in place is difficult to measure ($S/N=0.07$), so, we think that signals from true fluorescence can be ignored in this experiment.) The signal-to-noise ratio in these measurements was substantial (about 3) so that in situations where scattering measurements are more convenient than absorption measurements, this signal might be useful for monitoring membrane potential. These scattering changes could lead to artifacts in fluorescence if the barrier filter (filter 2) does not block the scattered light. But, because the barrier filters that we used in fluorescence measurements blocked more than 99.5% of the scattered light, when an appropriate barrier filter was inserted, interference from the scattering change was reduced to a level small compared to the fluorescence signals reported in Table 2.

Time Courses

Knowledge of the time course of the absorption, fluorescence, and birefringence signals in response to a step in potential may provide information about their molecular origins. Since the absorption, fluorescence, and birefringence changes found with dye I were all linearly dependent

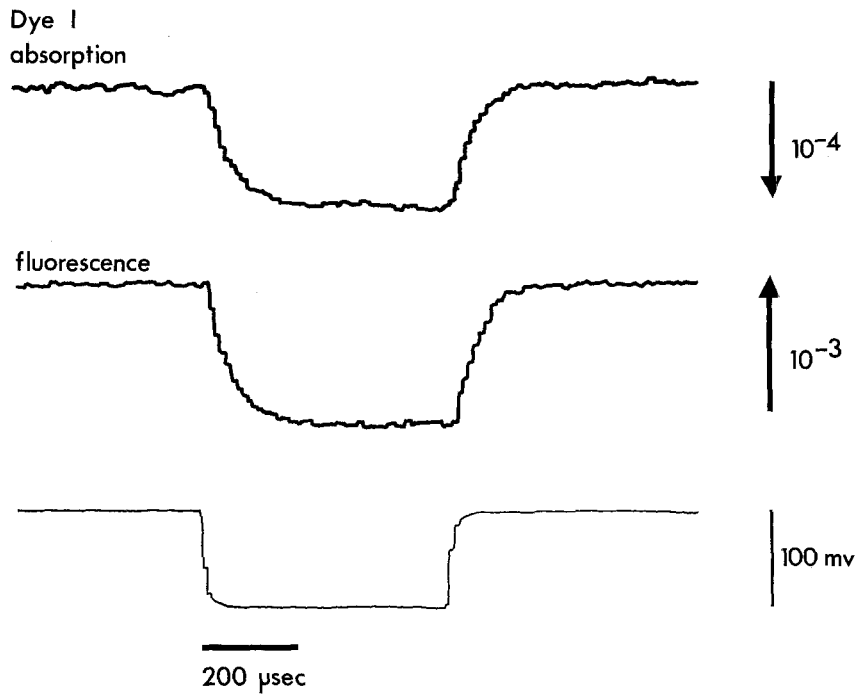

Fig. 9. Simultaneous measurement of absorption (top trace) and fluorescence (middle trace) during a 100 mV hyperpolarizing step (bottom trace) in an axon stained with dye I. When corrected for differences in the time constant of the light measuring system, the absorption and fluorescence changes were found to occur with the same time course. Filter 1 had a peak transmission at 570 nm, the barrier filter (filter 2) was Schott RG610 glass; 512 sweeps were averaged. The response time constant of the light measuring systems was 7 μsec for the absorption measurement and 13 μsec for the fluorescence measurement. Chamber temperature, 13 °C. The inward current at the end of the 100 mV depolarizing step was 0.1 mA/cm^2. In Figs. 9 and 10 the direction of the vertical arrow to the right of the fluorescence traces represents the direction of an increase in fluorescence; the size of the arrow represents the stated value of the change in fluorescence divided by the resting fluorescence that resulted from staining the axon. The axon was stained in a 0.1 mg/ml solution of the dye

upon membrane potential, it is possible that the three signals are different expressions of the same change in the membrane-dye complex. Thus, it was important to know if the signals occurred with the same time course. Accordingly, simultaneous absorption and fluorescence measurements were made using a relatively fast sweep and a lower temperature (13 °C). The results of such an experiment using incident light of 570 nm are shown in Fig. 9. Both the absorption and fluorescence changes were so rapid that accurate values for the time course could only be obtained after correction for the light measuring system (7 μsec, absorption;

13 μsec fluorescence) and the time constant of the change in membrane potential (15 μsec). After correction for these effects it was found that the time course of the absorption and fluorescence changes both lagged behind the potential by a single exponential with a time constant of 30 ± 3 μsec. Similarly, the absorption increase at 570 nm and the decrease at 530 nm measured with dye I had the same time course. In addition, the birefringence change found with dye I also occurred rapidly ($t < 50$ μsec at room temperature). Thus the time courses of these signals were similar, consistent with the hypothesis that all three had the same origin.

The time constants necessary to describe the absorption changes of dyes XVII, XVIII, 489 and 457 and the fluorescence changes of dyes 366, 368, 369 and 128 were less than 10 μsec at room temperature and could not be measured with our apparatus. In one experiment the time constant of the absorption change of the oxonol dye, XX, increased from 21 μsec at 23 °C to 32 μsec at 13 °C, a Q_{10} for the rate constant of 1.5.

Slow components. Not all signals had time courses that could be approximated by a single exponential. Fig. 10 compares the absorption change (top trace) of the cyanine dye, XIX, with its fluorescence change (bottom trace) measured simultaneously. On this time scale, the time course of the absorption change was too fast to be measured and there was no indication of more than one component. However, the time course of the fluorescence change was clearly different and cannot be fitted with a single exponential. Its time course can be approximated by the sum of two exponentials, one with a time constant of less than 100 μsec and a second with a time constant of 10 msec. Slow components were also seen in the birefringence signal. In experiments where relatively large concentrations of the oxonol dye, XXI, were used, the fluorescence signal had slow components while the absorption and birefringence signals, measured at the same time, did not. In addition, with several dyes that did exhibit both fast and slow components in their absorption signal, the wavelength dependence of the slow component differed from the wavelength dependence of the fast signal. Thus it seems likely that the fast and slow components result from different mechanisms. In one experiment (dye XIX), the slow component had a small temperature dependence, $Q_{10} = 1.2$.

Even though our experiments provide only preliminary information, it seems that the existence of slow components in the optical signal

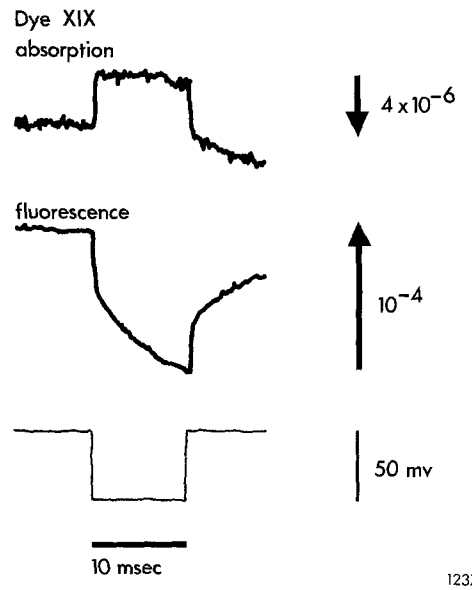

Fig. 10. Comparison of the absorption change (top trace) and the fluorescence change (middle trace) of an axon stained with dye XIX during a 10 msec hyperpolarizing potential step (bottom trace). The absorption change was essentially complete within 100 μsec of the beginning of the potential step, while the fluorescence continued to change throughout the hyperpolarization and had not returned to the baseline 30 msec after the end of the hyperpolarization. Filter 1 had a peak transmission at 660 nm. The barrier filter (filter 2) was Schott RG695 glass. 512 sweeps were averaged; the time constants of the light measuring systems were 60 μsec. The current density at the end of the 50 mV hyperpolarizing step was less than 0.1 mA/cm^2. A saturated solution of dye XIX in sea water was prepared at 60 °C. The axon was stained in a 1:4 dilution of this solution after it had cooled to 30 °C

is related to the structure of the dye. The cyanine dye, XIX, is positively charged at neutral pH and that charge is delocalized; the dye should be considered approximately as an equilibrium mixture between the two resonance structures where the positive charge is on either of the two nitrogen atoms. The analogues IV and 323, having only distributed charges, also had slow components while an additional analogue, XVIII, with two sulfonates had only fast components when the same concentration of dye was used. Similarly, dye 187 is an analogue of the oxonol, XXI, which has, in addition to the delocalized charge, a localized charge on a carboxylate (187) group. The fluorescence changes of XXI had slow components which were not seen with 187. Thus the presence of a localized charge usually led to a reduction or elimination of slow components. At the concentrations used for the experiments in Table 2 only the cyanine, XIX, and oxonol, XXI, had slow components.

Concentration. The existence of slow components often depended on the concentration of dye in the incubation solution. When the axon was incubated with a 5 μg/ml solution of the oxonol, XXI, the fluorescence signal-to-noise ratio was small, 0.2, and no slow component was observed. However, when the axon was incubated with a 200 μg/ml solution of the dye, the signal-to-noise ratio was greater than 5 and a slow component with a time constant of 10 msec made up about half of the signal during a 3 msec step. With dyes I and XVII, incubation at the highest concentrations used (0.2 mg/ml, I; 1.0 mg/ml, XVII) sometimes led to slow signals.

In two experiments the effect of concentration on the time course of the fast component of the fluorescence change of dye I was determined. The time course was more rapid when higher concentrations of dye were used. With one axon, incubation in a 5 μg/ml solution of dye resulted in a fluorescence change which lagged behind the potential with a time constant of 70 μsec at room temperature. Reincubation in a 100 μg/ml solution led to a time constant of less than 10 μsec. Since the bound dye did not readily wash-out, it was not possible to do a bracket experiment at low concentration, but we think the reduced time constant is not due to a change in the axon's condition since deterioration always led to longer time constants.

Dye Added Internally

Because of our interest in finding dyes that would be useful in monitoring membrane potential when added to neuronal membranes from the outside, only a few experiments were carried out on dyes that were microinjected into the axoplasm. With one exception, the absorption, fluorescence and birefringence signals that were obtained with dyes added internally were similar to those obtained with dyes added to the outside. For example, the absorption signal of the merocyanine-rhodanine, XVII, added to the inside was fast, having a time constant of less than 10 μsec; it had a wavelength dependence similar to that shown in Fig. 6*A*, the absorption change at 660 nm was very dichroic while that at 750 nm was not (compare with Fig. 6*B*). However the direction of the absorption changes found when this dye was added internally was always opposite to that found when the dye was added externally. The same was true for both the absorption and fluorescence signals of dye I, the only other dye with a localized charge that we tried on both sides. The finding that the signals obtained with dyes XVII and I were reversed in direction,

but similar in nature, when added to opposite sides of the membrane would be explained if there were equivalent sites on both membrane faces and the dyes were relatively impermeant. The signals obtained with four dyes which had only delocalized charge, XIX, XX, XXI and 366, were always in the same direction whether initially added to the outside or the inside of the axon membrane. These results would be explained if dyes with only delocalized charges are relatively permeant so that they can occupy the same position in the membrane independent of the side to which they were added. Thus, in addition to the effects of a localized charge in reducing slow components, the presence of a localized negative charge also seems to reduce the membrane permeability of the dye. Both results are consistent with the findings of Waggoner *et al.* (1977) and Waggoner, Sirkin, Tolles and Wang (1975) on black lipid membranes.

Discussion

Measurements carried out during action potentials and voltage clamp steps in squid axons, (e.g., Figs. 2, 3 and 4) provided evidence that the changes in extrinsic absorption, fluorescence, and birefringence were related to changes in membrane potential. The time courses of the intensity changes were similar during hyperpolarizing and depolarizing voltage clamp steps for every dye that was examined. However, even though there was no indication of components in any of the signals that were related to ionic currents or membrane conductance, because of uncertainties in making the proper compensation for the series resistance (Hodgkin, Huxley & Katz, 1952) with the apparatus we used, our ability to detect small components that were dependent on current or conductance was poor. We estimate that any signals related to current or conductance were less than 20% of the total signal measured during an action potential. When the membrane potential is near the resting potential, the membrane resistance is about 100 times greater than the sum of all other resistances between internal and external electrodes. Thus, 99% of the voltage drop during a hyperpolarizing step will appear across the membrane, only 1% appears across the axoplasm, Schwann cell, and sea water. (Hodgkin *et al.*, 1952). If one assumes a thickness of 50 Å for the membrane, then the change in voltage gradient across the membrane for a 50 mV hyperpolarization is 10^5 V/cm. Assuming a Schwann cell thickness of 5 μm, the voltage gradient across the Schwann cell is about 1 V/cm. Since the gradient across the membrane is about

10^5 larger than that across the Schwann cell, it seems likely that the rapid changes in fluorescence, absorption and birefringence originate from dye molecules that are in, or very close to, the axon membrane.

Mechanism. Sims *et al.* (1974) suggested that a change in membrane potential shifted the partition between cyanine dye in solution and dye associated with red cells, and the resulting changes in concentration caused a shift in the relative amounts of monomers and dimers (or higher aggregates) of the dye. Since the monomers and dimers have different absorption and fluorescence spectra, such a shift could explain the potential dependent changes in absorption and fluorescence they observed. We think that the absorption and fluorescence changes found with dye I (Fig. 7) can also be explained by a shift in monomer-dimer equilibrium, but we suggest the possibility that the signals result from a change in monomer-dimer equilibrium of dye that is *bound* to the axon membrane. The spectrum of the absorption change of dye I (Fig. 7*A*) is consistent with a monomer-dimer hypothesis. If the dimer has a large absorption peak at 530 nm and a smaller one at 630 nm and the monomer absorbs predominantly at 570 nm, then if a depolarization of the membrane caused a shift in the equilibrium towards the monomer and away from the dimer, the triphasic spectrum of the absorption signal of dye I would result. Such spectra for monomers and dimers of cyanine dyes were observed in aqueous solution (West & Pierce, 1965). Using a similar spectroscopic procedure the existence of membrane *bound* dimers has been disclosed by titrating a vesicle preparation with dye I (A. Grinvald, W.N. Ross, A.S. Waggoner, B.M. Salzberg and L.B. Cohen, *unpublished results*). (If the absorption change of dye I had resulted from a simple potential dependent displacement of an absorption band to a longer wavelength, only a diphasic spectrum would be predicted and the decrease at 630 nm would not be explained.) Furthermore, if the monomer is much more fluorescent than the dimer (Lavorel, 1957; West & Pierce, 1965), then a depolarization that shifted the equilibrium toward the monomer could lead to an increase in fluorescence at all excitation wavelengths. Since such an increase in fluorescence is observed, a potential dependent shift in monomer-dimer equilibrium could explain both the absorption and fluorescence signals found with dye I. A single explanation for the absorption and fluorescence signals would require that they have the same time course and potential dependence; these requirements are fulfilled. In addition, from an analysis of dimerization reactions (Eigen &

de Maeyer, 1963) it is expected that the rate of change of monomer-dimer equilibrium would be faster at higher dye concentrations and this was observed with dye I. However, the observation that both the fluorescence excitation spectra (ΔF *vs.* excitation wavelength) and the absorption spectra (ΔA *vs.* wavelength) are concentration dependent, and in addition that the excitation spectrum is also dependent on the emission wavelength implies that the situation is considerably more complicated than the one expected from the simplest two-state monomer-dimer hypothesis. A possible explanation for the observed results should postulate heterogeneity in the population of bound monomers and dimers, or the involvement of multimers in the process. The existence of some quenching mechanism of monomers' fluorescence at relatively high concentration, presumably via energy transfer from monomers to the weakly fluorescent dimers, is also required to explain the excitation spectra.

For the merocyanine-rhodanine dye, XVII, the absorption change is in the same direction at all wavelengths (Fig. 6*A*) suggesting that this signal may have different origins than the signal found with dye I. However, the spectrum obtained with light polarized perpendicular to the axon's axis is triphasic like that of dye I. Further experiments will be needed to determine the mechanism responsible for the signal found with dye XVII.

The finding that the absorption signals were dependent upon the plane of polarization of the incident light (Figs. 6*B* and 7*B*) implies that the magnitude or orientation of the absorption transition moments of some dye molecules must be altered when membrane potential changes. A reorientation could arise in two ways. If the orientations of monomer and dimer transition moments were different because monomer and dimer species bind to the membrane differently, or because dimerization itself results in an altered transition moment, then a shift in relative amounts of monomers and dimers would by itself result in a change in net transition moment. Alternatively, a reorientation would be obtained if the change in membrane potential caused a rotation of one or both of the species. Since no experiments have been done that would distinguish among these mechanisms, the conclusion that the dye molecules rotate (Warashina & Tasaki, 1975; Tasaki *et al.*, 1976; Tasaki & Warashina, 1976) seems premature. The absorption spectra of the monomer, dimer and higher aggregates of dyes I and XVII on the membrane have not been determined so the amount of resting orientation or the amount of rotation needed to explain the results obtained in Figs. 6*B* and 7*B*

cannot be specified, but it is clear that the same quantitative explanation cannot work for both dyes.

Signal size. Optical measurements of membrane potential using dyes that we described earlier (Cohen *et al.*, 1974) have been carried out in several different preparations (for reviews *see* Waggoner, 1976; Cohen & Salzberg, 1977). In terms of signal size, two very different kinds of results have been obtained. In experiments on suspensions of cells or cell organelles, where the total membrane area was large and the response time constant of the optical signal was in the range of 1–10 sec, the measured signals were relatively large, having a $\Delta I/I_r$ of about 1%/mV. This kind of signal was found using many cyanine dyes having only delocalized charges but not with a cyanine dye that also had localized charges (Sims *et al.*, 1974). Thus there was a correlation between dyes which gave large signals in red blood cell experiments and dyes with slow components in experiments on squid axons. Since signals of 1%/mV are easy to measure, any improvement in signal size that might be obtained by using dyes reported in this paper would not be important. On the other hand, in experiments on individual neurons or muscle fibers, where the membrane area is small and the response time constant of the optical signal is less than 10 μsec, the measured signals were relatively small, a $\Delta I/I_r$ of generally not more than 0.1%/mV. Since such signals are difficult to measure, the larger signal-to-noise ratios found with the dyes described in Table 2 should provide a substantial benefit. Fig. 11, a photograph of a single oscilloscope sweep, illustrates a simultaneous optical and electrode measurement of membrane potential during an action potential in a squid axon. The optical and electrode measurement can only be distinguished because a high frequency cut off filter was used in the optical measurement (top trace) to reduce the noise, and therefore the optical signal appears slower than the electrode measurement (bottom trace).

The improvement in signal-to-noise ratio in experiments on giant axons has continued steadily since 1970. The factors by which the signal increased in subsequent years were 2, 5, 1.6, 2 and 2. This steady progress suggests that even larger signals may be found in the future. Although the largest signal-to-noise ratio measured in our extrinsic birefringence experiments was only 5, only a few dyes were tried. A birefringence measurement might be advantageous in some situations because the signal occurs at wavelengths where the dye does not absorb, thereby eliminating any photodynamic damage and allowing a wide choice of wavelengths

Dye XVII

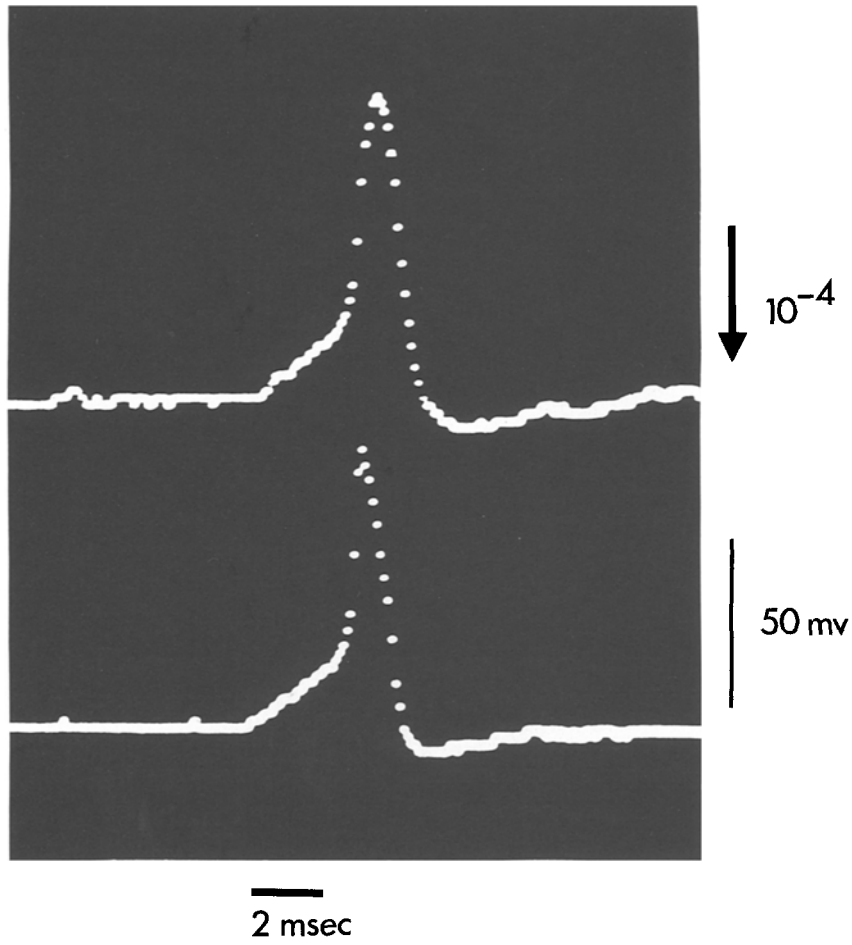

Fig. 11. Absorption change during an action potential of an axon stained with dye XVII. A single sweep was photographed from the Biomac cathode ray tube; no averaging was used. Filter 1 had a peak transmission of 750 nm. The response time constant of the light measuring system was 170 μsec. The axon was stained in a 0.1 mg/ml solution of the dye

that would avoid possible interference from intrinsic pigmentation. In preparations with high optical density, the intrinsic scattering signal may be useful.

The photodynamic damage associated with dye I caused difficulty in some preparations (Salzberg *et al.*, 1973; Oetliker *et al.*, 1975; Vergara & Bezanilla, 1976) but not in others (Salama & Morad, 1976). Hoff-

man and Laris (1974) also found no detectable damage in their experiments with red blood cells, using the cyanine dye, 72. Differences in incident light intensity probably explains part of the difference in the amount of damage. In our experiments on giant axons, the incident light intensity was 100 mW/cm^2 while in the experiments of Salama and Morad it was only 0.1–1.0 mW/cm^2. Similarly, in the experiments of Hoffman and Laris, the incident intensity was relatively low, 0.3 mW/cm^2. (In addition, from the results presented in Fig. 5, one would expect less damage with the cyanine dye used by Hoffman and Laris.) In any case, a discussion of the problem of photodynamic damage associated with dye I now seems moot, because the other dyes shown in Table 2 are at least 10 times less phototoxic than dye I (Fig. 5), and the damage associated with the best absorption dye, XVII, was so small that none was detected in experiments on leech segmental ganglia and frog skeletal muscle fibers.

We are especially grateful to Nippon Kankoh-Shikiso Kenkyusho, Ltd., for synthesizing dyes at our request and we thank Eastman Research Laboratories, G.A.F. Corp., Ilford, Ltd., Parke, Davis & Company, the Polaroid Corp., Xerox Corp., the Minnesota Mining and Manufacturing Company, Dr. J.W. Hauser and Dr. S.V. Levin for providing several of the dyes used in this paper. Drs. S.M. Baylor, H. Oetliker and W.K. Chandler kindly called our attention to a possible dye related birefringence signal that they found in experiments on frog muscle fibers, and we belatedly thank Dr. J. Yguerabide for pointing out the use of deoxygenation to block photodynamic damage. We thank Drs. B. Chance and E.M. Kosower for helpful suggestions during the course of the experiments. We are indebted to the director and staff of the Marine Biological Laboratory for their assistance. This work was supported by U.S. Public Health Service grants NS 08437 and NS 10489, from the National Institute of Communicative and Neurological Diseases and Stroke, an NIH postdoctoral fellowship 1 F22 NS-00927 to W.N.R. and a long-term EMBO Fellowship to A.G.

Appendix

Fluorescence and Absorption Changes of Additional Dyes Applied Externally to Squid Giant Axons

The signal-to-noise ratio of the change in fluorescence and absorption for a single 50-mV voltage-clamp step and the source of the dye according to the list in Table 1 are given in parentheses. Because of interference from the light scattering changes that occur in unstained axons, it was difficult to measure absorption changes with signal-to-noise ratios less than 0.04. When values less than 0.04 were obtained, they were recorded as no change (n.c.). The classification and nomenclature of most of the dyes conform to that of Hamer (1964). Within groups, the dyes are listed so that similar structures are near one another. Structural formulae are available from the authors. Dyes from Nippon Kankoh-Shikiso Kenkyusho, Ltd., Okayama, Japan (NK) are designated by the catalogue number in the company's organic chemical list (1969), and supplement (1974). The signal to noise ratio for absorption is given in italics.

Cyanine Dyes

Oxacyanines: 282. 3-benzyl-3′-ethyl-oxacarbocyanine iodide (1.1, NK-1416); 283. 3,3′-diethyl-5,5′ diphenyl-*meso*-ethyl-oxacarbocyanine iodide (0.1, NK-1088); 284. 3,3′-diethyl-*meso*-ethyl-oxacarbocyanine iodide (0.5, NK-736); 285. 3,3′-dimethyl-α,α-(p-methoxy-phenoxy)-oxacarbocyanine iodide (n.c., NK-1213); 286. 3,3′-diethyl-α-cyano-oxacarbocyanine iodide (n.c., NK-1425); 287. 3,3′-dipropyl-oxadicarbocyanine iodide (2.5, H); 288. 3,3′-dihexyl-oxadicarbocyanine iodide (0.75, H).

Thiacyanines: 72. 3,3′-dipropyl-thiadicarbocyanine iodide; (0.03, *1.0,* H); 78. anhydro-3,3′-di-γ-sulfopropyl-thiadicarbocyanine hydroxide (0.2, *0.2,* NK-2011); 83. 3,3′-diethyl-*meso*-phenyl-thiacarbocyanine iodide (1.8, *0.4,* NK-1507); 289. 3,3′-diethyl-6,6′-di-iodo-*meso*-methyl-thiacarbocyanine iodide (n.c., GA); 290. anhydro-3-γ-sulfopropyl-3′-(γ-trimethylammonium bromide)-propyl-*meso*-methyl-thiacarbocyanine hydroxide (0.1, Z); 291. 3,3′-bis-(β-hydroxyethyl)-5,5′-dichloride-*meso*-methyl-thiacarbocyanine iodide (n.c., GA); 292. 3,3′-dimethyl-α,α′-diphenoxy-thiacarbocyanine iodide (n.c., NK-1070); 293. 3,3′-dimethyl-*meso*-(2,3-dimethyl-1-phenyl-4(1H)-pyrazolyl-5-one)thiacarbocyanine iodide (0.5., IL); 294. 3,3′-diethyl-*meso*-styryl-thiacarbocyanine iodide (0.5, NK-93); 295. 3,3′-dimethyl-α,α′-vinylene-thiacarbocyanine iodide (n.c., IL); 296. 3,3′-dimethyl-α,α-ethylene-thiacarbocyanine iodide (2.5, GA); 297. 3,3′-diethyl-*meso*-methyl-thiacarbocyanine iodide (0.4, GA); 298. 3-ethyl-3′-methyl-*meso*-ethoxy-thiacarbocyanine iodide (0.5, GA); 299. 3-ethyl-3′-b-hydroxyethyl-*meso*-methyl-thiacarbocyanine iodide (0.5, GA); 300. 3,3′-dimethyl-α,α′-o-phenylene thiacarbocyanine iodide (0.05, IL); 301. 3,3′,α,α′-tetramethyl-thiacrabocyanine iodide (n.c., GA); 302. 3,3′-diethyl-4,5,4′,5′-dibenzo-*meso*-phenyl-thiacarbocyanine iodide (n.c., *n.c.,* NK-1632); 303. 4,5,4′,5′-dibenzo-3′-ethyl-3-γ-sulfopropyl-*meso*-ethyl-thiacarbocyanine iodide (0.1, *0.1,* NK-2069); 304. 3,3′-di(β-carboxyethyl)-thiadicarbocyanine iodide (0.3, Z); 305. 3-3′-diethyl-β,β′-neopentylene-thiadicarbocyanine iodide (4.0, *5.3,* H, NK-1836); 306. anhydro-3-γ-sulfopropyl-1-ethyl-6-methyl-β,β′-neopentylene-thiadicarbocyanine hydroxide (0.6, *n.c.,* NK-2070); 307. 3,3′-diethyl-β,β′-(2-phenylpropylene)-thiadicarbocyanine iodide (n.c., IL); 308. 3,3′-diethyl-thia-β,δ-(neopentylene) tricarbocyanine iodide (1, *1.5,* H); 309. 3,3′-diethyl-5,5′-dichloro-thia(γ,γ′-dimethylene)-*meso*-diphenylamino tricarbocyanine perchlorate (n.c., *n.c.,* M); 310. 5,6,5′6′-dibenzo-3,3′-bis(γ-acetoxypropyl)-γ,γ′-dimethylene-*meso*-diphenylamino-thiatricarbocyanine perchlorate (*1.1,* M).

Indocyanines: IV. 1,1′-diethyl-3,3,3′3′-tetramethyl-indotricarbocyanine iodide (3.0, *1.6,* NK-1414); 122. 1,3,3,1′,3′,3′-hexamethyl-indodicarbocyanine iodide (2.5, *4,0,* NK 529); 312. 1,3,3,1′,3′,3′-hexamethyl-5,5′-dinitro-indocarbocyanine (*p*-toluene sulfonate) (0.3, Z); 313. 3,3,3′,3′-tetramethyl-1,1′-bis(γ-hydroxypropyl)-indocarbocyanine iodide (0.5, *1.0,* NK-1883); 314. anhydro-1,1′-di-γ-sulfopropyl-3,3,3′,3′-tetramethyl-5,5′-dinitro-indocarbocyanine hydroxide (0.2, *0.3,* NK-2063); 315. 1,3,3,1′,3′,3′-hexamethyl-indocarbocyanine (benzoate) (0.3, NK-419); 316. 1,3,3,1′,3′3′-hexamethyl-5,5′-dinitro-indodicarbocyanine iodide (0.04, *0.3,* NK-A); 317. 1,1′-diethyl-3,3,3′,3′-tetramethyl-indodicarbocyanine iodide (1.7, *0.1,* H); 318. 3,3,3′,3′-tetramethyl-1,1′-dipropyl-indodicarbocyanine iodide (2.7, *1,* H); 319. 1,1′-dibutyl-3,3,3′,3′-tetramethyl-indodicarbocyanine iodide (2, H); 320. 1,1′-diheptyl-3,3,3′,3′-tetramethyl-indodicarbocyanine iodide (n.c., H); 321. 1,1′-dicarboxymethyl-3,3,3′,3′-tetramethyl-*meso*-bromo-indodicarbocyanine iodide (1.5, NK-1681); 322. 1,1′-di-δ-sodium-sulfobutyl-3,3,3′,3′-tetramethyl-4,5,4′,5′-dibenzo-indodicarbocyanine iodide (4.5, *12,* NK-1841); 323. 1,3,3,1′,3′,3′-hexamethyl-indotricarbocyanine iodide (3, *n.c.,* NK-2029); 324. 3,3,3′,3′-tetramethyl-1,1′-dipropyl-indotricarbocyanine iodide (3.3, H); 325. 1,1′-diethyl-3,3′-di-(spiro-cyclohexane) indotricarbocyanine (0.03, *0.07,* H). 326. anhydro-1,1′-di-γ-sulfopropyl-3,3,3′,3′-tetramethyl-indotricarbocyanine hydroxide (0.2, *0.4,* NK-1967); 327. 4,5,4′,5′-dibenzo-1,3,3,1′,3′,3′-hexamethyl-indotricarbocyanine iodide (n.c., *n.c.,* NK-2014); 328. an-

hydro-1-(γ-sulfopropyl)-1′-(γ-triethyl ammonium-sulfopropyl)-4,5,4′,5′-dibenzo-3,3,3′,3′-tetramethyl-γ,γ′-dimethylene-*meso*-(4-carbethoxy-1-piperazinyl) indotricarbocyanine hydroxide (*0.3,* M).

Quinolino or Pyrido-cyanines: 110. 1,1′-diethyl-2,2′-carbocyanine iodide (0.01, *0.06,* C); 329. 1,1′-dimethyl-*meso*-phenyl-2,2′-carbocyanine iodide (0.8, *2.5,* NK-1865); 330. 1,1′-diethyl-6,6′-diethoxy-7,7′-bis-isopropyl-2,2′-carbocyanine iodide (n.c., *n.c.,* NK-1762). 331. 1,1′-diallyl-6,6′-dimethyl-2,2′-carbocyanine iodide (0.6, L); 332. 1,6,1′,6′-tetramethyl-2,2′-carbocyanine iodide (n.c., PD). 333. 1,1′-di-(β-carboxyethyl)-4,4′-carbocyanine iodide (n.c., *n.c.,* NK-1753); 334. 1,1′-di-β-ethoxyethyl)-4,4′-carbocyanine iodide (0.4, PD); 335. 1,1′-dimethyl-α,α′-vinylene-4,4′-carbocyanine iodide (0.05, IL); 336. 1,1′-diethyl-4,4′-pyridocarbocyanine iodide (n.c., *n.c.,* NK-2079); 337. 1,1′-dimethyl-4,4′-pyridocarbocyanine iodide (n.c., NK-492); 338. 1,1′-diethyl-2,2′-dimethyl-4,4′-pyrido-carbocyanine iodide (n.c., NK-491); 339. 1,1′-diethyl-2,4′-carbocyanine iodide (0.3, NK-138); 340. 1,1′-diethyl-6-dimethylamino-2-4′-carbocyanine iodide (n.c., NK-1271); 341. 1′-ethyl-1,2-dimethyl-2-pyrido-2′-carbocyanine iodide (0.09, NK-335); 342. 1,1′-diethyl-6,6′-diethoxy-7,7′-bis-isopropyl-*meso*-chloro-2,2′-dicarbocyanine iodide (0.1, *0.05,* NK-1805); 343. 1,1′-diethyl-*meso*-nitro-4,4′-dicarbocyanine iodide (n.c., *n.c.,* NK-1944); 344. 1,1′-(γ-sodium sulfopropyl)-4,4′-pyridotricarbocyanine iodide (0.4, *n.c.,* H).

Other cyanines: 128. 1′-ethyl-1,3,3-trimethylindo-4′-carbocyanine iodide (3, *0.06,* NK-323); 345. 4-β-[2,5-dimethyl-1-phenyl-pyrrolyl(3)]-vinyl-1-methylquinolinium iodide (0.4, PD); 346. 4-β-[2,5-dimethyl-1-phenyl-pyrrolyl(3)]-vinyl-6-methoxy-1-methylquinolinium iodide (n.c., PD); 347. 2-β-[2,5-dimethyl-1-phenyl-pyrrolyl(3)]-vinyl-1-dodecyl-6-methylquinolinium iodide (0.06, PD); 348. 2-β-[2,5-dimethyl-1-phenyl-pyrrolyl(3)]-vinyl-5-methoxy-1-methylquinolinium iodide (0.03, PD); 349. 2-β-[2,5-dimethyl-1-phenyl-pyrrolyl(3)]-vinyl-6-dimethylamino-1-methylquinolinium iodide (0.06, PD); 350. 2-β-[1-heptyl-2,5-dimethyl-pyrrolyl(3)]-vinyl-1,6-dimethylquinolinium iodide (0.2, PD); 351. 2-β-[2-methyl-indolyl(3)]-vinyl-1,6-dimethylquinolinium iodide (n.c., PD); 352. 3,3′-diethyl-4,5,4′,5′-tetraphenyl-*meso*-chloro-thiazolodicarbocyanine iodide (n.c., NK-1254); 353. 3,3′-diethyl-thiazolotricarbocyanine iodide (0.3, H); 354. 3,4,3′-4′-tetramethyl-5′-carbethoxy-thiazolocarbocyanine iodide (1.2, NK-317); 355. 3′-benzyl-3,4′-dimethyl-4,5-benzo-thiathiazolocarbocyanine iodide (n.c., GA); 356. 3-ethyl-3,4′-dimethyl-thiathiazolocarbocyanine iodide (n.c., NK-318); 357. 5′-carboxy-3-ethyl-3′,4′-dimethyl-thiathiazolocarbocyanine iodide (n.c., NK-1464); 358. 4,5-benzo-3,3′-dimethyl-4′,5′-diphenyl-thiathiazolinocarbocyanine iodide (n.c., GA); 359. 3,3′-diethyl-5′-methyl-thiathiazolinocarbocyanine iodide (0.18, NK-1058); 360. 1′,3-diethyl-4,5-diphenyl-thiazolo-4′-carbocyanine iodide (0.1, NK-1209); 361. 1′-ethyl-3-heptyl-4-methyl-thiazolo-2′-carbocyanine iodide (0.05, NK-304); 362. 2-carbethoxy-3,4-dimethyl-1-ethyl-thiazolo-4′-carbocyanine iodide (0.2, NK-320); 363. 1′,3-diethyl-thia-4′-carbocyanine iodide (0.16, NK-321); 364. 2-[β-(1-piperidyl)-vinyl]-3,4-dimethyl-thiazolium iodide (n.c., NK-620); 365. 2-[β-(diphenylamino)-vinyl]-3,4-dimethyl-thiazolium iodide (n.c., NK-359); 366. 1,3′-diethyl-3,3,5′,6′-tetramethyl-indoxacarbocyanine iodide (4.0, *0.5,* AA); 367. 3′-ethyl-1,3,3-trimethyl-indoxacarbocyanine iodide (1.2, GA); 368. 4,5,4′5′-dibenzo-1,3′-diethyl-3,3-dimethyl-indoxacarbocyanine iodide (6.0, *0.3,* AA); 369. 4,5-benzo-3,3,5′,6′-tetramethyl-1,3′-diethyl-indoxacarbocyanine iodide (4.0, *1.0,* AA); 370. 2-[6-dimethyl-amino)-1,3,5-hexatrienyl]-3,3-dimethylindolenine methiodide (0.5, *0.7,* NK-2044); 371. 3,3′-diethyl-6′-diethylamino-4,5-diphenyl-oxazolino-thiacarbocyanine iodide (n.c., GA); 372. 3,3′-diethyl-6′-methyloxa-α-azathiacarbocyanine iodide (0.05, GA); 373. 3,3′-diethyl-oxathiacarbocyanine iodide (0.4, NK-720); 374. anhydro-3-γ-sulfopropyl-3′-ethyl-5-phenyl-oxathiacarbocyanine hydroxide (0.4, NK-1490); 375. anhydro-3′-γ-sulfopropyl)-3-ethyl-5-phenyl-oxathiacarbocyanine hydroxide (n.c., NK-1518); 376. 1′-3-diethyl-oxa-2′-carbocyanine iodide (0.06, NK-740); 377. 1′,3-diethyl-oxa-4′-carbocyanine iodide (0.4, NK-741); 378. 3,3′,4,4′-tetramethyl-

oxazolocarbocyanine iodide (n.c., NK-307); 379. 2-[3-(5-methyl-2-(1.3.4-oxadiazolyl))-2-propenyl-idene]-3-ethyl-5,6-dimethyl-benzoxazoline (0.2, GA); 380. 4-[β-(diphenylamino)-vinyl]-1-ethylquinolinium iodide (n.c., NK-700); 381. 3,3′-diethyl-5,5′-dimethyl-selenacarbocyanine iodide (0.3, *0.2,* NK-1090); 382. anhydro-3,3′-di-γ-sulfopropyl-selenacarbocyanine hydroxide (0.06, GA); 383. 3-ethyl-3′-γ-sulfopropyl-*meso*-methyl-selenacarbocyanine iodide (n.c., GA); 384. 3,3′-diethyl-*meso*-methyl-selenacarbocyanine iodide (0.4, *0.3,* NK-1091); 385. 3,3′-diethyl-selenadicarbocyanine iodide (0.1, *n.c.,* NK-1590); 386. 3,3′-diethyl-selenatricarbocyanine iodide (0.05, *n.c.,* NK-747); 387. 1,3′-diethyl-selena-4′-carbocyanine iodide (0.1, *n.c.,* NK-744); 388. 1,3,1′,3′-tetraethyl-5,6,5′,6′-tetrachloro-benzimidazolocarbocyanine iodide (n.c., NK-1420); 389. 1,3,1′,3′-tetraethyl-benzimidazolocarbocyanine iodide (n.c., NK-1094); 390. 2-[β-(dimethylamino)-vinyl]-1,3-diethyl-benzimidazolium iodide (n.c., NK-1556); 391. 5-aceto-1,3-diethyl-3′-methyl-benzimidazolo-oxacarbocyanine iodide (n.c., NK-1201); 392. 1,3,3,1′,3′3′-hexamethyl-(3H)-isopyrrolo-[2,3,-b]pyridocarbocyanine iodide (0.15, IL); 393. 2-[3-(3-methyl-2-benzothiazolinylidene)-1-propenyl]-3,3,4,7-tetramethyl-isopyrrolo[2,3,-b]pyridinium iodide (0.5, IL); 394. 2-[-3-(3-methyl-2-benzoxazolinylidene)-1-propenyl]-3,3,4,7-tetramethyl-isopyrrolo[2,3-b]pyridinium iodide (0.5, IL); 395. 7,7′-diethyl-3,3,3′,3′-tetramethyl-2-(3H)-isopyrrolo[2,3-b]pyrido carbocyanine iodide (0.6, IL); 396. 1,1′-diethyl-3,3′-dimethyl-pyridazino-carbocyanine iodide (n.c., *n.c.,* NK-1846); 397. 1,3,3,3′-tetramethyl-indoxatricarbocyanine iodide (3.5, *1.5,* NK-2029).

Trinuclear cyanines: 398. 6,6′-diethoxy-1,1′-dimethyl-*meso*-(6-ethoxy-2(1H)-quinolylidene-methine)-2,2′-carbocyanine iodide (n.c., NK-226); 399. 1,1′-diethyl-*meso*-[1-ethyl-4(1H)-quinolylidene-methine] 4,4′-carbocyanine (n.c., NK-224); 400. 2,2′-bis-[(1,3,3,1′,3′,3′-hexamethyl)-indolenine-trimethine]-1,1′-diethyl-bisbenzothiazole (bis-toluen sulfonate) (2.5, Z).

Merocyanine Dyes

Benzoxazole merocyanines: I. 5-[(3-sodium sulfopropyl-2(3H)-benzoxazolylidene)-2-butenylidene]-1,3-dibutyl-2-thiobarbituric acid (5.5, *10,* H); XIV. 5-[(3-γ-sodium sulfopropyl-2(3H)-benzoxazolylidene)-2,4-hexadienylidene]-1-3-diethyl-2-thiobarbituric acid (0.9, *0.2,* H); 137. 5-[(3-γ-sodium sulfopropyl-2(3H)-benzoxazolylidene)-2-butenylidene]-1,3-dipentyl-2-thiobarbituric acid (4.9, *8,* H); 138. 5-[(3-γ-sodium sulfopropyl-2(3H)-benzoxazolylidene)-2-butenylidene]-1,3-dihexyl-2-thiobarbituric acid (4.5, *13,* H); 401. 5-(3-ethyl-5,6-dimethyl-2-(3H)-benzoxazolylidene)-ethylidene]-1,3-diphenyl-2-thiohydantoin (n.c., NK-1113); 402. 5-[(3-δ-sodium sulfobutyl)-2(3H)-benzoxazolylidene)-2-butenylidene]-1,3-dipropyl-2-thiobarbituric acid (1.5, *0.4,* H); 403. 5-[(3-δ-sodium sulfobutyl-2(3H)-benzoxazolylidene)-2-butenylidene]-1,3-dibutyl-2-thiobarbituric acid (11.0, *7.0,* H); 404. 5-[(3-γ-sodium sulfopropyl-2(3H)-benzoxazolylidene)-2-butenylidene]-1,3-diallyl-2-thiobarbituric acid (0.08, *0.2,* H); 405. 5-[(3-γ-sodium-sulfopropyl-2(3H)-benzoxazolylidene)-1,3-neopentylene-2-butenylidene]-1,3-dibutyl-2-thiobarbituric acid (8.0, *6.0,* H); 406. 5[3-γ-sodium sulfopropyl-2(3H)-benzoxazolylidene)-2-butenylidene]-1,3-dibutylbarbituric acid (0.06, *0.07,* G); 407. 3-[(3-γ-sodium sulfopropyl-2(3H)-benzoxazolylidene-2-butenylidene]-6-methyl-2,3-dihydropyrane-2,4-dione (n.c., G); 408. 3-[3-γ-sodium sulfopropyl-2(3H)-benzoxazolylidene)-2-butenylidene]-5,6-benzo-2,3-dihydropyrane-2,4-dione) (n.c., G); 409. 4-[3-γ-sodium sulfopropyl-2(3H)-benzoxazolylidene)-2-butenylidene]-3-phenyl-5(4H)-isoxazolone (n.c., G); 410. 4-[(3-γ-sodium sulfopropyl-2(3H)-benzoxazolylidene)-2-butenylidene]-1,1-dimethyl-3,5-cyclohexanedione (n.c., G).

Indolenine merocyanines. IX. 5-[(3,3-dimethyl-1-γ-sodium sulfopropyl-2(3H)-indolylidene)-2-butenylidene]-1,3-dibutyl-2-thiobarbituric acid (7.8, *5.3,* H); 136. 2-[(1,3,3-trimethyl-2(3H)-

indolylidene)-ethylidene]-3(2H)-thianaphthenone (0.5, *0.23*, NK-1183); 411. 5-[(3-γ-sodium-sulfopropyl-2(3H)-benzoxazolylidene)2-butenylidene]-2,2-dimethyl 4,6-dioxo-1,3-dioxane; (n.c., G); 412. 5-[(1-γ-sodium sulfopropyl-3-spiro cyclohexane-2(3H)-indolylidene)-2-butenylidene]-1,3-dibutyl-2-thiobarbituric acid (8.5, *1.5*, H); 413. 4-[3,3-dimethyl-1-γ-sodium sulfopropyl-2(3H)-indolylindene)-2-butenylidene]-3-phenyl-5(4H)-isoxazolone (0.1, *1.5*, NK-B); 414. 5-[3,3-dimethyl-1-δ-sulfobutyl-2(3H)-indolylidene)-2-butenylidene]-1,3-dibutyl-2-thiobarbituric acid (5.0, *6.0*, NK-E); 415. 5-[3,3-dimethyl-1-γ-sodium sulfopropyl-5-nitro-2(3H)-indolylidene)-2-butenylidene]-1,3-dibutyl-2-thiobarbituric acid (2.0, *0.5*, NK-D);

Benzothiazolo merocyanines: XV. 5-[(3-γ-sodium sulfopropyl-2(3H)-benzothiazolylidene)-2-butenylidene]-1,3-dibutyl-2-thiobarbituric acid (1.1, *0.8*, H); 416. 5-[(3-γ-sodium-sulfopropyl-4,5-benzo-2(3H)-benzothiazolylidene)-ethylidene]-3-ethyl-1-phenyl-2-thiohydantoin (0.08, Z). 417. α-[(3-ethyl-2(3H)-benzothiazolylidene)-2,4-hexadienylidene]-α-cyano methylacetate (0.5, NK-1583).

Other merocyanines: III. 5-[(3-γ-sodium sulfopropyl-2(3H)-thiazolinylidene)-2-butenylidene]-1,3-dibutyl-2-thiobarbituric acid (2.9, H); 418. 1-[(1-methyl-4(1H) quinolylidene)-ethylidene]-4-cyclohexadienone (0.03, XE); 419. 5-[(1-γ-sodium sulfopropyl-4(1H)-pyridylidene) 2-butenylidene]-1,3-dibutyl-2-thiobarbituric acid (1.7, *0.15*, H); 420. 5-[(1-γ-sulfopropyl-4(1H) quinolylidene)-2-butenylidene]-1,3-dibutyl-2-thiobarbituric acid (0.5, *0.7*, H); 421. 5-[(3-γ-sulfopropyl-2-thiazolinylidene)-2-butenylidene]-1,3-dibutyl-2-thiobarbituric acid (0.5, *0.5*, NK-C); 422. 2-[(1-methyl-4(1H)-pyridylidene) 2,4-hexadienyl-idene]-1,3-indanedione (*n.c.*, *0.06*, H); 423. 2-[(1-γ-triethylammonium bromide-propyl-4-(1H)-pyridylidene) 2,4-hexadienylidene]-1,3-indanedione (n.c., *n.c.*, H); 424. 2-[(1-γ-sodium-sulfopropyl-4(1H)-pyridylidene) 2,4-hexadienylidene]-1,3-indanedione (n.c., *0.2*, H); 425. 5-[(1-γ-sodium sulfopropyl-4(1H)-pyridylidene) 2,4-hexadienylidene]-1,3-dibutyl-2-thiobarbituric acid (1.5, *0.5*, H); 426. 5-[(1-methyl-4(1H)-pyridylidene)-2,4-hexadienylidene]-1,3-diethyl-2-thiobarbituric acid 0.2, *0.3*, H); 427. 5-[(1-γ-sodium sulfopropyl-4(1H)-pyridylidene)-2,4-hexadienylidene]-1,3-diethyl-2-thiobarbituric acid (0.5, *0.5*, H); 428. 5-[(1-γ-triethylammonium bromide-propyl-4(1H)-pyridylidene) 2,4-hexadienylidene]-1,3-diethyl-2-thiobarbituric acid (0.4., *0.01*, H); 429. 4-[(1-ethyl-4(1H)-pyridylidene)-2-4-hexadienylidene]-1,1-dimethyl-3,5-cyclohexanedione (n.c., *n.c.*, H); 430. 4-[(1-methyl-4(1H)-pyridylidene) 2,4-hexadienylidene]-3-phenyl-5(4H)-isoxazolone (0.1, *0.3*, NK-2031).

Merocyanine rhodanine dyes: 173. 5-[(3,3-dimethyl-1-γ-sodium sulfopropyl-2(3H)-indolylidene)-2-butenylidene]-3-ethyl rhodanine (0.4, *1.5*, H); 178. 5-[(1-ethyl-4(1H)-quinolylidene)-ethylidene]-3-carboxymethyl-rhodanine (n.c., *0.6*, NK-1663); 431. 5-[(1-ethyl-4(1H)-quinolylidene)-ethylidene]-3-ethyl rhodanine (0.02, *0.06*, NK-1069); 432. 5-[(1-methyl-4(1H)-quinolylidene)-ethylidene]-3-phenyl rhodanine (n.c., *0.06*, NK-912); 433. 5-[(1-γ-sodium sulfopropyl-4-(1H)-quinolylidene)-ethylidene]-3-ethyl rhodanine (0.9, *15.0*, NK-1936); 434. 5-[(1-ethyl-2(1H)-quinolylidene)-ethylidene]-3-sodium carboxymethyl rhodanine (n.c., *n.c.*, NK-2088); 435. 5-[(1-γ-potassium sulfopropyl-2(1H)-quinolylidene)-α-methyl-ethylidene]-3-ethyl rhodanine (*0.1*, Z); *436.* 5-[(1-γ-sodium sulfopropyl-4(1H)-pyridylidene)-ethylidene]-3-ethyl rhodanine (n.c., *n.c.*, H); 437. 5-[(3-ethyl-2(3H)-benzothiazolylidene)-ethylidene]-3-β-sodium sulfoethyl rhodanine (n.c., *n.c.*, NK-2065); 438. 5-[(3-ethyl-2(3H)-benzothiazolylidene)-α-methyl-ethylidene]-3-ethyl rhodanine (0.2, *0.1*, Z); 439. 5-[(3-ethyl-2(3H)-benzothiozolylidene)-ethylidene]-3-carboxylmethyl rhodanine (n.c., Z); 440. 5-[(3-ethyl-2(3H)-benzothiazolylidene)-β-methyl-ethylidene]-3-ethyl-rhodanine (0.08, Z); 441. 5-[(3-methyl-2(3H)-benzothiazolylidene)-ethylidene]-3-ethyl rhodanine (n.c., Z); 442. 5-[2(3,5-dimethyl-thiazolidylidene)-ethylidene]-3-ethyl rhodanine (0.07, *1.7*, NK-1778); 443. 5-[2-(3,5-dimethyl thiazolidylidene)-ethylidene]-rhodanine (n.c., *n.c.*, NK-1777); 444. 5-[(3-ethyl-4-methyl-5-carbethoxy-2(3H)-thiazolylidene)-ethylidene]-3-ethyl rhodanine (n.c., *n.c.*, NK-1459); 445.

5-[(1,3-diethyl-2(1H)-benzimidazolylidene)-ethylidene]-3-ethyl rhodanine (n.c., *n.c.,* NK-1222); 446. 5-[(1-ethyl-3-methyl-6-(1H)-pyridazinylidene)-ethylidene]-3-ethyl rhodanine (n.c., *0.3,* NK-1848); 447. 5-[(3-γ-sodium sulfopyrpyl-5-phenyl-2(3H)-benzoxazolylidene)-ethylidene]-3-β-sodium carboxyethyl rhodanine (n.c., *n.c.,* NK-2062); 448. 5-[(3-γ-sodium sulfopropyl-5-phenyl-2(3H)-benzoxazolylidene)-ethylidene]-3-ethyl rhodanine (1.4, *0.6,* NK-2071); 449. 5-[(3-ethyl-2(3H)-benzoselenazolylidene)-ethylidene]-3-ethyl rhodanine (n.c., NK-1248); 450. 5-[(1-ethyl-4-methyl-(1H)-pyrimido[1,2-a]benzimidazole-2-ylide)-ethylidene]-3-ethyl rhodanine (n.c., Z); 451. 5-[2-(3,3,7-trimethyl-2-pyrrolino[2,3-b] pyridinium-ylidene)-ethylidene]-3-ethyl-rhodanine iodide (0.05, IL); 452. 5-[(1-γ-sodium sulfopropyl-4(1H)-quinolylidene)-2-butenylidene]-3-allyl rhodanine (−, *20.0,* H); 453. 5-[(1-γ-sodium-sulfopropyl-4(1H)-quinolylidene)-2-butenylidene]-3-hexyl rhodanine (−, *0.6,* H); 454. 5-[(1-γ-sodium sulfopropyl-4(1H)-quinolylidene)-2-butenylidene]-3-phenyl rhodanine (−, *4.0,* H); 455. 5-[(1-γ-sodium sulfopropyl-4(1H)-quinolylidene)-2-butenylidene]-3-butyl rhodanine (−, *5.0,* H); 456. 5-[(1-ethyl-4(1H)-quinolylidene)-2-butenylidene]-3-ethyl rhodanine (0.03, *0.4,* NK-1318); 457. 5-[(1-γ-triethylammonium-sulfopropyl-4(1H)-quinolylidene)-2-butenylidene]-3-methyl rhodanine (0.2, *12.0,* H); 458. 5-[(1-γ-sodium-sulfopropyl-4(1H)-quinolylidene)-2-butenylidene]-3-propyl rhodanine (−, *20,* H); 459. 5-[(1-γ-sodium sulfopropyl-2(1H)-quinolylidene)-2-butenylidene]-3-ethyl rhodanine (n.c., *0.5,* NK-1935); 460. 5-[(1-ethyl-4(1H)pyridylidene)-2-butenylidene]-3-ethyl rhodanine (n.c., *n.c.,* NK-1311); 461. 5-[(3-β-sodium-carboxyethyl-6-methyl-2(3H)-benzothiazolylidene)-2-butenylidene]-3-β-sodium carboxyethyl rhodanine (n.c., *n.c.,* NK-1901); 462. 5-[(3-γ-sodium-sulfopropyl-2(3H)-benzothiazolylidene)-2-butenylidene]-3-ethyl rhodanine (0.1, *0.4,* NK-1934); 463. 5-[(3-pentyl-2(3H)-benzothiazolylidene)-2-butenylidene]-3-β-sodium carboxyethyl rhodanine (0.08, *n.c.,* NK-2052); 464. 5-[(3,4-dimethyl-5-carboxy-2(3H)-thiazolylidene)-2-butenylidene]-3-ethyl rhodanine (0.03, NK-1469); 465. 5-(2(3H)-benzoxazolylidene-2-butenylidene)-3-ethyl rhodanine (0.06, NK-1672); 466. 5-[(4,5-benzo-3-ethyl-2(3H)-benzoxazolylidene)-2-(α-methyl) butenylidene]-3-ethyl rhodanine (n.c., Z); 467. 5-[(3-ethyl-2(3H)-benzothiazolylidene)-2,4-hexadienylidene]-3-ethyl rhodanine (n.c., NK-1575); 468. 5-[(1-γ-sodium sulfopropyl-4(1H)-quinolylidene)-2,4-hexadienylidene]-3-ethyl rhodanine (0.04, *3.0,* H).

Rhodacyanines. 469. 5-[(5,6-dimethyl, 3-propyl-2(3H)-benzolthiazolylidene) ethylidene]-2-[(4,5-diphenyl-2-thiazolylethiodide)-methine] 3-allyl-4-oxothiazolidine (n.c., *n.c.,* NK-1954); 470. 5-[(3-ethyl-2(3H) benzothiazolylidene)-1-methyl-ethylidene]-2-[4,5-diphenyl 2-thiazolinyl ethio-toluene sulfonate-methine] 3-ethyl-thiazolidine (n.c., Z).

Oxonol Dyes

193. Bis-[1,3-diethyl-barbituric acid-(5)]-pentamethinoxonol (0.75, *0.5,* NK-2040); 471. bis-[3-phenyl-rhodanine-(5)] methinoxonol (n.c., NK-913); 472. bis-[3-γ-sodium sulfopropyl-rhodanine-(5)] methinoxonol (n.c., *n.c.,* NK-1941); 473. bis-[1,3-dipropyl-barbituric acid-(5)]-trimethinoxonol (0.6, *0.3,* H); 474. bis-[1,3-dibutyl-barbituric acid-(5)]-trimethinoxonol (0.7, *0.1,* H); 475. bis-[1,3-dihexyl-barbituric acid-(5)]-trimethinoxonol (0.15, *0.05,* H); 476. bis-[1,3-dibutyl-2-thiobarbituric acid-(5)]-trimethinoxonol (0.3, H); 477. bis-[(3H)-thianaphthenone-(2)]-trimethinoxonol (0.06, NK-1742); 478. bis-[barbituric acid-(5)]-pentamethinoxonol (0.1, *n.c.,* NK-2041); 479. bis-[1,3-dimethyl-barbituric acid-(5)]-pentamethinoxonol (0.06, H); 480. bis-[1,3-dipropyl-barbituric acid-(5)]-pentamethinoxonol (4.0, H); 482. bis[1,3-dipenthyl-barbituric acid-(5)]-pentamethinoxonol (0.2, H); 483. bis-[1,3-dihexyl-barbituric acid-(5)]-pentamethinoxonol (n.c., H); 484. bis-[1,3-dioctyl-barbituric acid-(5)]-pentamethinoxonol (n.c., H); 485. bis-[1,3-dimethyl-2-thiobarbituric acid-(5)]-pentamethinoxonol (1.3, *n.c.,* H); 486. bis-[1,3-dibutyl-2-thiobarbituric acid-(5)]-pentamethinoxonol (n.c.,

H); 487. Bis-[1,3-diethyl-2-thiobarbituric acid-(5)]-pentamethinoxonol (2.0, *n.c.*, H); 489. bis-[1-phenyl-(3-carbobutoxy-5-pyrazolone-(4)]-pentamethinoxonol (1.2, *7.0*, Z); 490. bis-[1-phenyl-3-(carbethoxy-methylene)-5-pyrazolone-(4)]-pentamethinoxonol (0.1, *0.1*, H); 491. bis-[1-phenyl-3-carbo-β-hydroxyethoxy)-5-pyrazolone-(4)]-pentamethinoxonol (n.c., *0.5*, Z); 492. bis-[1-phenyl-3-methyl-5-pyrazolone-(4)]-pentamethinoxonol (0.2, *0.2*, H); 493. bis-[1-(p-(N-pentyl-sulfonamido phenyl)]-3-carbo-(α-hydroxy-ethoxy)-5-pyrazolone-(4)]-pentamethinoxonol (n.c., *n.c.*, Z); 494. bis-[3-phenyl-5(4H)-isoxazolone-(4)]-pentamethinoxonol (0.8, *2.0*, NK-2047); 495. bis-[1-*p*-sulfophenyl-3-methyl-5-pyrazolone-(4)]-pentamethinoxonol (0.1, *0.4*, NK-1939); 496. bis-[1-(*p*-N-pentyl-sulfonamido phenyl)-3-carbethoxy-5-pyrazolone-(4)]-pentamethinoxonol (0.4, *0.4*, Z); 497. bis-[3-ethyl-rhodanine-(5)]-pentamethinoxonol (n.c., *n.c.*, NK-2095); 498. bis-[1,3-indanedione-(2)]-pentamethinoxonol (0.12, H); 499. bis-[1-indanone-(2)]-pentamethinoxonol (n.c., H); 500. bis-[5,5-dimethyl-1,3-cyclo-hexanedione-(2)]-pentamethinoxonol (0.04, H).

Styryl Dyes

501. 2-(p-dimethylaminostyryl)-6-dimethylamino-1-ethyl-quinolinium iodide (n.c., *n.c.*, NK-1867); 502. 2-(p-dimethylaminostyryl)-6-ethoxy-quinoline (0.08, NK-1629); 503. 2-(p-dimethylaminostyryl)-1-methyl-quinolinium p-toluenesulfonate (0.25, H); 504. 4-(p-dimethylamino-styryl)-1-pentyl-quinolinium iodide (0.4, NK-282); 505. 4-(m-nitrostyryl)-1-ethyl-quinolinium iodide (n.c., NK-113); 506. 2-(p-dimethylaminostyryl)-3,3-trimethyl-1-ethyl-pseudoindolium iodide (n.c., *n.c.*, NK-1977); 507. 2-(p-dimethylaminostyryl)-1,3,3,-trimethyl-pseudoindolium iodide (n.c., *n.c.*, NK-2043); 508. 2-(p-hydroxystyryl)-1,3,3-trimethyl-pseudoindolium iodide (n.c., *n.c.*, NK-1637); 509. 2-(p-hydroxystyryl)-1,3,3-trimethyl-4-amino-pseudoindolium iodide (n.c., *n.c.*, NK-1654); 510. 2-(p-nitrostyryl)-3,4,5-trimethyl-oxazolium iodide (n.c., NK-985); 511. anhydro-5-carboxy-2-(p-dimethylaminostyryl)-1-ethyl-benzothiazolium hydroxide (n.c., *n.c.*, NK-2089); 512. anhydro-γ-sulfopropyl-2-(p-dimethylaminostyryl)-4-methyl-thiazolium hydroxide (n.c., *n.c.*, NK-2054); 513. 6-(p-dimethylaminostyryl)-1-ethyl-3-methyl-pyridazinium iodide (2.5, *1.5*, NK-1847); 514. 4-(*p*-dimethyl aminobenzylidene)-10-methyl-1,2,3,4,tetrahydroacridinium iodide (0.3, PD); 515. 2-[4-(p-dimethylaminophenyl)-1,3-butadienyl]-1-heptyl-quinolinium iodide (0.6, NK-384); 516. 2[4(*p*-dimethylaminophenyl)-1,3 butadienyl]-6,7-benzo-3-ethyl benzothiazolium iodide (0.05, *0.1*, NK-1823).

Other Structural Types

Aminovinyls. 517. 2-[β-(-5-bromo-pyridyl, (2)-amino]-vinyl-3-ethyl-1-methyl-pyridinium iodide (n.c., *n.c.*, NK-1833).

Benzals. 518. 2-[p-dimethylaminobenzylidene]-3-thianaphthenone (0.11, NK-1184); 519. 5-[p-methylaminobenzylidene]-3-phenyl rhodanine (n.c., NK-1106); 520. 5-[5-(p-dimethylaminophenyl) 1,3-neopentylene-2,4-pentadienylidene]-1,3-diethyl-2-thiobarbituric acid (0.3, *0.3*, H); 521. 5-[3-(p-dimethylaminophenyl)-2-propenylidene]-1,3-diethyl 2-thiobarbituric acid (0.5, *0.5*, NK-2090); 522. 5-[3-(p-dimethylaminophenyl)-2-propenylidene]-1,3-dibutyl barbituric acid (0.07, G).

Triphenylmethane. 523. chlorophenol red (n.c., *n.c.*, C); 524. Coomassie brilliant blue R (0.5, *0.1*, M); 525. phenol red (n.c., *0.16*, C).

Amino azines. 13. Neutral red (0.3, *0.4*, B,C); 526. Magdala red (0.06, D); 527. iodo methoxy neutral red (0.05, *0.15*, JH); 528. de amino neutral red (0.12, *0.15*, JH).

Acridines. 1. Acridine orange (0.3, *0.8*, K); 529. iodoproflavine (0.05, *0.05*, JH); 530. iodoacridine orange (0.4, *0.75*, JH).

Oxazins. 19. Brilliant cresyl blue (0.03, *0.1*, D,F); 24. Nile blue A (0.8, *0.4*, D).

Xanthenes. 30. Rhodamine B (0.5, *0.13*, D); 31. Rhodamine 3B (1.6, *0.06*, N).

Other types. 69. J. Red-Brown (no potential); 69' Talapena Red Chandler (bald zero); 531. Arsenazo III (−, *n.c.*, L); 532. Chlorophosphonazo III (−, *0.2*, F); 533. Coumarin 30 (0.4, *0.08*, M); 534. Coumarin 6 (n.c., *0.1*, M); 535. 5-[β-(1-ethyl-4(1H)quinolylidene)-ethylidene-(3-ethyl-2-thiazolidinylidene-4-one)]-3-ethyl-rhodanine (0.2, *n.c.*, NK-2096); 536. 5-[β-(3-ethyl-2(3H)-benzothiazolylidene)-ethylidene (3-ethyl-2-thiazolidylidene-4-one)]-3-ethyl-rhodanine (0.05, *0.08*, NK-2097); 537. 5-[β-(1-ethyl-2(3H) benzoxazolylidene)-ethylidene]-2-[(4,5-diphenyl-2-thiazolyl-ethiodide)-methine]-3-ethyl-oxazolidine-4-one (0.3, *0.5*, NK-2022); 538. 1-(1-tetrahydroquinolyl-4-acetoxy-1,3,5-heptatrienylidene)-tetra-hydroquinolinium iodide (n.c., NK-1109); 539. 2-(β-ferrocenylvinyl) 1,3,3-trimethyl-pseudoindolium iodide (n.c., Z); 540. 2-(β-ferrocenyl-vinyl)-3-ethyl-benzothiazolium ethiodide (n.c., Z); 541. 2-[β-thioxo-β-(N-phenyl-acetamido)ethylidene]-1-ethyl-2(3H)-benzoselenazole (n.c., NK-1073); 542. 2,4,6-tri-p-tolyl-1-(3,5-diphenyl-4-hydroxy phenyl) pyridinium iodide (n.c., XE); 543. 4,4′-bis{4-(3-sulfanilino)-6-[bis(2-hydroxyethyl)-amino]1,3,5-triazin-2-yl amino}-stilbene 2,2′-disulfonic acid tetrasodium salt (n.c., *n.c.*, CG); 544. Helogen blue (−, *0.02*, SL).

References

Arvanitaki, A., Chalazonitis, N. 1961. Excitatory and inhibitory processes initiated by light and infra-red radiations in single excitable nerve cells (giant ganglion cells of *Aplysia*). *In:* Nervous Inhibition. E. Florey, editor. p. 194. Pergamon Press, New York

Baylor, S.M., Oetliker, H. 1975. Birefringence experiments on isolated skeletal muscle fibers suggest a possible signal from the sarcoplasmic reticulum. *Nature (London)* **253**:97

Bennett, H.S. 1950. The microscopical investigation of biological materials with polarized light. *In:* McClung's Handbook of Microscopical Technique. R.M. Jones, editor. Paul B. Hoeber, New York

Braddick, H.J.J. 1960. Photoelectric photometry. *Rep. Prog. Phys.* **23**:154

Brooker, L.G.S., Keyes, G.H., Sprague, R.H., Dyke, R.H. van, Lare, E. van, Zandt, G. van, White, F.L., Cressman, H.W.J., Dent, S.G., Jr. 1956. Color and constitution. X. Absorption of the merocyanines. *J. Am. Chem. Soc.* **73**:5332

Cohen, L.B., Hille, B., Keynes, R.D. 1969. Light scattering and birefringence changes during activity in the electric organ of *Electrophorus electricus*. *J. Physiol (London)* **203**:489

Cohen, L.B., Hille, B., Keynes, R.D. 1970. Changes in axon birefringence during the action potential. *J. Physiol. (London)* **211**:495

Cohen, L.B., Hille, B., Keynes, R.D., Landowne, D., Rojas, E. 1971. Analysis of the potential-dependent changes in optical retardation in the squid giant axon. *J. Physiol. (London)* **218**:205

Cohen, L.B., Keynes, R.D., Hille, B. 1968. Light scattering and birefringence changes during nerve activity. *Nature (London)* **218**:438

Cohen, L.B., Keynes, R.D., Landowne, D. 1972. Changes in light scattering that accompany the action potential in squid giant axons: Potential-dependent components. *J. Physiol. (London)* **224**:701

Cohen, L.B., Landowne, D., Shrivastav, B.B., Ritchie, J.M. 1970. Changes in fluorescence of squid axons during activity. *Biol. Bull. Woods Hole* **139**:418

Cohen, L.B., Salzberg, B.M. 1977. Optical measurements of membrane potential. *Rev. Physiol. Biochem. Pharmacol. (in press)*

Cohen, L.B., Salzberg, B.M., Davila, H.V., Ross, W.N., Landowne, D., Waggoner, A.S., Wang, C.H. 1974. Changes in axon fluorescence during activity: Molecular probes of membrane potential. *J. Membrane Biol.* **19**:1

Conti, F., Tasaki, I. 1970. Changes in extrinsic fluorescence in squid axons during voltage-clamp. *Science* **169**:1322

Davila, H.V., Cohen, L.B., Salzberg, B.M., Shrivastav, B.B. 1974. Changes in ANS and TNS fluorescence in giant axons from *Loligo*. *J. Membrane Biol.* **15**:29

Davila, H.V., Salzberg, B.M., Cohen, L.B., Waggoner, A.S. 1973. A large change in axon fluorescence that provides a promising method for measuring membrane potential. *Nature New Biol.* **241**:159

Eigen, M., Maeyer, L. de 1963. Relaxation methods. *In:* Technique of Organic Chemistry. A. Weissberger, editor. Vol. VIII, part II, p. 903. John Wiley and Son, New York

Frederiq, E., Houssier, C. 1973. Electric Dichroism and Electric Birefringence. Clarendon Press, Oxford

Hamer, F.M. 1964. The Cyanine Dyes and Related Components. John Wiley and Son, New York

Hodgkin, A.L., Huxley, A.F. 1952. A quantitative description of membrane current and its application to conduction and excitation in nerve. *J. Physiol. (London)* **117**:500

Hodgkin, A.L., Huxley, A.F., Katz, B. 1952. Measurement of current-voltage relations in the membrane of the giant axon of *Loligo*. *J. Physiol. (London)* **116**:424

Hoffman, J.F., Laris, P.C. 1974. Determination of membrane potentials in human and *Amphiuma* red blood cells by means of a fluorescent probe. *J. Physiol. (London)* **239**:519

Houssier, C., Kuball, H.G. 1971. Electro-optical properties of nucleic acids and nucleoproteins. III. Kramers-Kronig relationships in linear birefringence and dichroism. Application to a DNA-Proflavine complex. *Biopolymers* **10**:2421

Keynes, R.D. 1963. Chloride in the squid giant axon. *J. Physiol. (London)* **169**:690

Lavorel, J. 1957. Influence of concentration on the absorption spectrum and the action spectrum of fluorescence of dye solutions. *J. Phys. Chem.* **61**:1600

Oetliker, H., Baylor, S.M., Chandler, W.K. 1975. Simultaneous changes in fluorescence and optical retardation in single muscle fibres during activity. *Nature (London)* **257**:693

Pooler, J. 1972. Photodynamic alteration of sodium currents in lobster axons. *J. Gen. Physiol.* **60**:367

Ross, W.N., Cohen, L.B., Salzberg, B.M., Kohn, N., Grinvald, A. 1975. Extrinsic birefringence and dichroism changes in squid giant axons. *Biol. Bull. Woods Hole* **149**:444

Ross, W.N., Salzberg, B.M., Cohen, L.B., Davila, H.V. 1974*a*. A large change in dye absorption during the action potential. *Biophys. J.* **14**:983

Ross, W.N., Salzberg, B.M., Cohen, L.B., Davila, H.V., Waggoner, A.S., Wang, C.H. 1974*b*. A large change in axon absorption during the action potential. *Biol. Bull. Woods Hole* **147**:496

Salama, G., Morad, M. 1976. Merocyanine 540 as an optical probe of transmembrane electrical activity in the heart. *Science* **191**:485

Salzberg, B.M., Cohen, L.B., Ross, W.N., Waggoner, A.S., Wang, C.H. 1976. New and more sensitive molecular probes of membrane potential: Simultaneous optical recordings from several cells in the central nervous system of the leech. *Biophys. J.* **16**:23*a*

Salzberg, B.M., Davila, H.V., Cohen, L.B. 1973. Optical recording of impulses in individual neurons of an invertebrate central nervous system. *Nature (London)* **246**:508

Schmitt, F.O., Bear, R.S. 1937. The optical properties of vertebrate nerve axons as related to fiber size. *J. Cell. Comp. Physiol.* **9**:261

Sims, P.J., Waggoner, A.S., Wang, C.H., Hoffman, J.F. 1974. Studies on the mechanism by which cyanine dyes measure membrane potential in red blood cells and phosphatidylcholine vesicles. *Biochemistry* **13**:3315

Tasaki, I., Warashina, A. 1975. Changes in light absorption, emission and energy transfer produced by electric stimulation of nerves labeled with fluorescent probes. *Proc. Jpn. Acad.* **51**:604

Tasaki, I., Warashina, A. 1976. Fast and slow rotation of dye molecules in squid axon membrane during excitation. *Proc. Jpn. Acad.* **52**:37

Tasaki, I., Warashina, A., Pant, H. 1976. Studies of light emission, absorption and energy transfer in nerve membranes labelled with fluorescent probes. *Biophys. Chem.* **4**:1

Tasaki, I., Watanabe, A., Sandlin, R., Carnay, L. 1968. Changes in fluorescence, turbidity and birefringence associated with nerve excitation. *Proc. Nat. Acad. Sci. USA* **61**:883

Vergara, J., Bezanilla, F. 1976. Fluorescence changes during electrical activity in frog muscle stained with merocyanine. *Nature (London)* **259**:684

Waggoner, A.S. 1976. Optical probes of membrane potential. *J. Membrane Biol.* **27**:317

Waggoner, A.S., Sirkin, D., Tolles, R.L., Wang, C.H. 1975. Rate of membrane penetration of potential sensitive dyes. *Biophys. J.* **15**:20*a*

Waggoner, A.S., Wang, C.H., Tolles, R.L. 1977. Mechanism of potential-dependent light absorption changes of lipid bilayer membranes in the presence of cyanine and oxonol dyes. *J. Membrane Biol.* **33**:109

Warashina, A., Tasaki, I. 1975. Evidence for rotation of dye molecules in membrane macromolecules associated with nerve excitation. *Proc. Jpn. Acad.* **51**:610

West, W., Pierce, S. 1965. The dimeric state of cyanine dyes. *J. Phys. Chem.* **69**:1894